

1 **Multi-millennial-scale solar activity and its lagged**
2 **influences on ~~continental-tropical~~ climate: Empirical &**
3 **tested evidence of recurrent cosmic and terrestrial patterns**

4 J. Sánchez-Sesma¹

5 [1]{ Instituto Mexicano de Tecnología del Agua, Mexico }

6 Correspondence to: J. Sánchez-Sesma (jsanchez@tlaloc.imta.mx)

7

8 **Abstract**

9 Solar activity (SA) oscillations over the past millennia are analyzed and extrapolated based on
10 reconstructed solar-related records. Here, simple recurrent models of SA signal are applied
11 and tested. The consequent results strongly suggest: a) the existence of multi-millennial
12 (~9500-yr) scale solar oscillations, and b) their persistence, over at least the last glacial-
13 interglacial cycle. This empirical modelling of solar recurrent oscillations has also provided a
14 consequent multi-millennial-scale experimental forecast, suggesting a solar decreasing trend
15 toward Grand (Super) Minimum conditions for the upcoming period, 2050-2250 AD (3750-
16 4450 AD). Also, a recurrent linear influence of solar variation on continental tropical climate
17 (CTC) has been assessed for the last 20 Kyr, and extrapolated for the next centuries. Taking
18 into account the importance of these estimated SA scenarios, a comparison is made with other
19 SA forecasts, and their possible associated astronomical forcing and influences on **past and**
20 **future ~~CTC~~ climate** discussed. **In four Appendixes, we provide further verification, testing,**
21 **and analysis of solar recurrent patterns since geological eras, their potential gravitational**
22 **forcing, the lagged responses of the Earth's climate system (ECS), and the sea level lagged**
23 **(by ~1550yr) response to tropical climate forcing.**

1 Duhau and Jager, 2010; Perry and Hsu, 2000). It should be noted that all proponents of
2 planetary forcing have forecasted a solar Grand Minimum for the upcoming decades, but one
3 of them has also forecasted a Super Minimum for the next centuries (Perry and Hsu, 2000). In
4 addition, during recent decades, statistical forecasts (with physically-based spectral
5 information of reconstructed records) of solar magnetic activity predict a clear decrease in
6 SA, reaching a minimum around 2100 AD (Steinhilber et al., 2013; hereafter S13; Velasco et
7 al., 2015).

8 It should also be noted that several recent studies have been devoted to reconstruct multi-
9 millennial-scale solar/climate related records. In relation to solar records, Steinhilber et al.
10 (2009; hereafter S09), Steinhilber et al., (2012; hereafter S12), Solanki et al., (2004; hereafter
11 S04), and Finkel and Nishiizumi (1997; hereafter FN97) have investigated isotopic
12 concentrations in ice-cores and tree-rings over the past 9,500, 9,500, 11,500, and 40,000
13 years, respectively, in order to estimate SA and/or related isotopic production. Another [two](#)
14 [isotopic reconstructions](#) by Stuverik-Storm et al. (2014; hereafter SS14), and [Adolphi et al.](#)
15 [\(2014; hereafter A14\)](#) have just provided detailed key information over 20 Kyr for the past
16 interglacial, or Eemian [period](#), more than 100,000 years ago, [and for the last deglaciation, over](#)
17 [8Kyr from 19 to 11 Kya, respectively.](#)

18 These different cosmogenic radionuclide-based reconstructions of SA present variations for
19 the past millennia, and as Muscheler and Heikkilä (2011) have pointed out, large uncertainties
20 appear in reconstructions of the solar modulation of galactic cosmic rays from different
21 proxies, ^{10}Be and ^{14}C , and of changes in the geomagnetic shielding influence. However,
22 these reconstructed records provide, especially when considered all together, the most
23 objective information as elements for detecting and eventually modelling and extrapolating
24 multi-millennial-scale solar oscillations, trends and absolute levels.

25 In terms of climate, and following Haigh (2011), who has pointed out that “it is now possible
26 to identify decadal and centennial signals of solar variability in climate data,” we have
27 complementarily analyzed one important tropical climate record: the reconstructed Congo
28 River basin surface air temperature (CRB-SAT) record, because it covers the last 25 Kyr
29 (Weijers et al., 2007; hereafter W07). This tropical climate variable is very important because
30 its location, at the center of tropical Africa, generates [a relative](#) [isolation](#) [from](#) [to](#) ocean
31 influences and thus enhances solar influences. This influence is known as continentality.

1 In addition to solar influences on climate, recent studies have highlighted the importance of
2 human activities, and suggest that **anthropogenic influences on global warming (GW) are**
3 **currently active**, imposing a projected change of 4 ± 2 °C by 2100 AD that seems to exceed
4 the maxima values estimated for the past millennia (IPCC, 2013). However, an understanding
5 of climate change remains incomplete because firstly, the main signals of climate **long-**
6 **term millennia-scale** forcings have not been well described, neither forecasted, and require
7 further work, with new methods and new data, as is the case for phenomena such as solar and
8 volcanic activity; secondly, paleoclimate studies have begun to consider **cosmoclimate**
9 approaches (Shaviv et al., 2014); thirdly, solar influence appears to be modulated by the
10 **thermo-haline circulation (THC)** that increased during the present interglacial (Piotrowski et
11 al., 2004); **and fourthly, the detected ECS lagged responses (analyzed in this work) in**
12 **different scales and regions of the world, would modify our conceptions of and approaches to**
13 **modelling climate processes.**

14 In this paper, we attempt to advance our knowledge of solar variability by considering
15 reconstructed records of **variables** related with SA over the last glacial cycle, from isotopic
16 information coming from ice-cores and tree-ring layers, reanalyzing them with a linear
17 modelling of oscillations with recurrent influences. This modelling is achieved through simple
18 analogues and Fourier series models. Tests of the proposed method and the detected low-
19 frequency solar signal, going back in time, are based on independent data. Finally, we discuss
20 the different oscillations detected, the confidence of our forecasts, some alternative forecast
21 methods, and astronomical information that suggests a possible planetary **gravitational** forcing
22 of SA by an unknown mechanism during the last millennia, and its past and future modulated
23 **and recurrent** influences on continental tropical climate (CTC) **and sea level. Further analysis**
24 **is provided in four Appendixes. Appendix A: Qualitative verification of total solar irradiance**
25 **(TSI) ~9.5Ky recurrent patterns with a bivalve population (BVpop) reconstructed from late**
26 **Miocene (~10.5Mya) data. Appendix B: Empirical evidence of a planetary gravitational**
27 **forcing of the ~9500yr total solar irradiance (TSI) recurrent pattern. Appendix C: Non-linear**
28 **lagged responses of the Earth's climate system (ECS): A power law, its verification, and an**
29 **example (Iron deposition in the south-western Pacific lags solar activity by ~1500 yrs).**
30 **Appendix D: Sea level lags (~1500 yr) tropical climate.**

31

1 1 Methodology

2 1.1 Data

3 In order to analyze solar/climate recurrent oscillatory patterns, six different reconstructed
4 forcing (five) and climate (one) proxy records of these oscillations are presented used.

5 We have analyzed five different sets of solar-related information. Firstly, total solar irradiance
6 (*TSI* or *S*, hereafter) reconstructed by S04, S09 and S12, based on the isotopic information of
7 ¹⁴C and ¹⁰Be, have recently provided records of SA anomalies for the last millennia. Figure 1a
8 displays S04, S09 and S12 reconstructed and intercalibrated values from 9450 BC to 1900
9 AD, from 7360 BC to 2009 AD, and from 7350 BC to 1988 AD, respectively. The variance
10 explanation (obtained as the square of the correlation coefficient multiplied by 100) between
11 S04&S09, S04&S12, and S09&S12 for decadal average records are of 52.7, 82.9 and 59.3 %,
12 respectively.

13 Secondly, there are three interesting and useful solar-related, ¹⁰Be isotope concentration
14 records from Greenland ice core, one covering the past 40 Kyr (FN97) and the, another
15 covering only 20 Kyr but located at belonging to the Eemian (SS14), and another covering
16 20-10 Kyr BP (A14). Figure 1b and Figure 1c display the information of ¹⁰Be FN97, SS14,
17 and A14 records.

18 Thirdly, we will look at a climate record for tropical areas for the last millennia, specifically
19 the Congo River basin surface air temperature (CRB-SAT) record, because it covers the last
20 25 Kyr and it is a continental tropical climate record obtained with a novel and promising
21 molecular technique (W07), based on changes in lipids associated with surface temperatures.
22 This CRB-SAT record (W07), or Tcrb, is relatively more solar-influenced than the rest non-
23 tropical areas of the world, because the latitudinal distribution of solar influences shows its
24 maximum in the tropics. Moreover, this record is also relatively less influenced by the ocean
25 than in coastal regions, because its signal is coming from the central tropical zone of Africa,
26 which is also isolated by topography. The detrended Tcrb information is displayed in Figure
27 1c, and presents higher oscillations in the glacial and deglacial periods with respect to those
28 corresponding to the Holocene.

29 Although oceanic influences on the Tcrb are minimal, Tcrb responses to SA should be
30 modulated during the interglacial differently due to the increasing intensity of THC that has
31 been reconstructed by Piotrowski et al. (2004), who pointed out: “From a minimum during the

1 Last Glacial Maximum (LGM), North Atlantic Deep Water (NADW) began to strengthen
2 between 18 and 17 Kyr cal. BP, approximately 2000–3000 years before the Bølling
3 warming.”

4 1.2 Modelling

5 To take into account different time-scale recurrences, the solar/climate, SC , variable can be
6 expressed with three models. One model is based on the Fourier Series (FS), another is based
7 on a linear transformation of the proxy variable values, and the last one is based on temporal
8 analogues.

9 The FS model can be written by means of:

$$10 \quad SC(t) = \sum_{j=1}^{N_{FS}} \left[a_j \cdot \sin\left(j \frac{2\pi(t)}{T}\right) + b_j \cdot \cos\left(j \frac{2\pi(t)}{T}\right) \right] + e_{FS}(t), \quad (1)$$

11 Here, T is the FS base period, N_{FS} represents the number of FS terms or harmonics, j is an
12 index component term, a and b are amplitudes, t is time, and $e_{FS}(t)$ is the error in this model.

13 Based on Piotrowski et al. (2004), and the changes of amplitude in the detrended CRB record,
14 the model for the lagged and modulated linear contribution of a proxy variable is proposed as
15 follows:

$$16 \quad SC(t) = M[\alpha_p P(t + \delta_p) + \beta_p(t - t_1) + \gamma_p] + e_p(t), \quad (2)$$

17 With $M=1$ for $0 < t < 10$ KyrBP, $M=1+0.133(t-10)$ for $10 < t < 17.5$ KyrBP, and $M=2$ for
18 $17.5 < t < 25$ KyrBP.

19 Here, $P(t)$ is the proxy variable, α_p is the amplification factor, β_p is the slope, δ_p is the lag,
20 γ_p is the additive constant, t_1 is the initial times for the modeled period, and $e_p(t)$ is the error
21 of this model.

22 The analogue model is defined as:

$$23 \quad SC(t) = \alpha_A SC(t + \delta_A) + \beta_A(t - t_1) + \gamma_A + e_A(t), \quad (3)$$

24 Here, α is the amplification factor, β is the slope, δ is the lag, γ is the additive constant, t_1 is
25 the initial times for the modeled period, and $e_A(t)$ is the analogue error of this model.

1 In all these models, parameters are estimated through iterative or multi-linear regression
2 processes that minimize the RMS values of errors.

3 Taking into account both the dating limitations and the approximated values provided by
4 proxy reconstructions, and instead of to developing statistical analysis, as convergence and
5 confidence level estimations, we prefer in this stage of research about climate recurrences, to
6 apply verification/replication of all of our findings with independent information in our
7 estimation processes and results. Future climate reconstructions with more accurate
8 information will provide further and refined statistical analysis.

9

10 **2 Results**

11 2.1 Long-term solar-activity recurrent patterns

12 In order to detect multi-millennia-scale recurrences and/or persistent oscillations in SA, we
13 need to analyze ^{10}Be information since it is a solar proxy variable and it is available over
14 longer periods than SA records (SS14). However, there are several ^{10}Be post-production and
15 fallout processes (i.e. residence time in the atmosphere, scavenging rate, troposphere-
16 stratosphere exchange, precipitation rate, etc.) that may alter the concentration found in the
17 ice archive (FN97; SS14).

18 Accepting that ^{10}Be concentration variability is influenced by climatic variability through
19 long-term variable trends and modulations, we propose to apply a homogenization process
20 based on statistics to the ^{10}Be (FN97) record. Firstly, a detrending process based on
21 polynomial expressions was applied. And secondly, a demodulation was applied in an attempt
22 to make the variance uniform. The consequent results show the ^{10}Be atmospheric signal of
23 this process with approximated recurrent oscillations with lags of 9.6 and 19.2 Kyr, which
24 are shown in the Supplementary Information (SI) Section 1 (SI-1).

25 The statistically detrended ^{10}Be FN97 record was modeled with a periodic FS function with
26 $N_{\text{FS}}=10$ that employed Eq. 1. After a minimization processes, a 9390 yr period, P, was found
27 and the corresponding model that explain 49.2 % of variance is displayed in Figure 2a.

28 It should be noted that the solar and climate recurrence periods evaluated with FS and
29 analogue techniques (shown in SI) have shown values of 9500 ± 100 yrs (~ 9.5 Kyr).

1 Before extrapolating the ^{10}Be ~9.5 Kyr recurrences to TSI, we applied a wavelet analysis to
2 the three TSI records. The TSI spectral results (see **SI-4**) show three main, significant
3 periodicities around 5000, 2400 and 900 years, and confirms the existence in **solar activity** of,
4 at least three **harmonics of the ~9.5 Kyr oscillations**.

5 2.2 Verification of the recurrences of the ^{10}Be ~9.5Ky patterns

6 Although this FS periodic ^{10}Be model is based only on the last 40 Kyr (see Figure 2b), it
7 was extrapolated to cover the last 130 Kyr, for comparison with other independent
8 information of ^{10}Be . A detailed comparison with the ^{10}Be SS14 record (in 5 parts) coming
9 from Greenland and the Eemian **period** is displayed in Figure 2c. The maximum **variance**
10 **explanation, of 18.4%**, corresponds to a temporal adjustment of 2.5 Kyr (a temporal bias
11 going back in time) of the SS14 dating. This temporal adjustment is justified because a similar
12 one, of 2.3 Kyr, is required by the SS14 18O record when it is compared with another
13 reconstruction from NGRIP Greenland ice-cores by Kindler et al. (2014; hereafter K14),
14 which is shown in **SI-2**. This comparison constitutes an important verification and test of the
15 proposed FS model.

16 In order to verify the detected recurrent patterns of ^{10}Be , we apply different homogenization
17 and extrapolation processes to FN97 data. Specifically, we follow the original calculations
18 made by FN97 and the suggestions provided by Dr. Nishiizumi (personal communication,
19 2014), and we have also calculated the atmospheric signal of ^{10}Be ($^{10}\text{Be}_{\text{Atm}}$) based on
20 accumulated snow (Cuffey and Clow, 1997) and the signal of ^{10}Be coming from the GISP2
21 ice core. Our normalizations, **which are devoted to eliminating high-frequency local climate**
22 **influences on the ^{10}Be signal**, have provided elements (records) to confirm the previous
23 results for the ~9.5 Kyr recurrence and a consequent **increase and diminishing of the $^{10}\text{Be}_A$**
24 **and TSI signals, respectively**, for the following centuries, as also shown in the SI-3.

25 We have also shown, in Appendix A, a qualitative verification of the total solar irradiance
26 (TSI) ~9.5Ky recurrent patterns with a bivalve population (BVpop) reconstructed from late
27 Miocene (~10.5Mya) data.

2.3 Empirical tests of the recurrence and potential mechanisms of TSI ~9.5Ky patterns.

Looking for physical basis and robust evidence of the detected recurrences, we have developed two qualitatively different tests of the multi-millennial recurrences of TSI: a test based on a suggested gravitational forcing, and a test based on the TSI (S04) and 10Be (A14) records.

The test, based on a physical mechanism, which develops a gravitational forcing analysis, is shown in Appendix B. It is an empirical analysis of the gravitational forcing due to lateral forces. Those lateral forces generate a low-frequency signal with a period of ~9500 yrs, preceding by ~6700 yrs, and is similar to the low-frequency solar activity. Additional analysis of a non-linear lagged response of TSI to gravitational forcing is analyzed and suggests a logarithmic model variation for different forcing periods.

The last test, which is based on a high-resolution independent and normalized 10Be record (A14), consists of an extrapolation backward in time of the TSI(S04) record [this record reconstructed sun-spot numbers or SSN], which is based on 14C records from well-dated tree-ring studies. First, a temporal bias correction, a 70-yr lag, was applied to the 10Be record to enhance the correlation with the 14C based TSI(S04) record without being extrapolated backward in time. After this adjustment, an application of the analogue model (a linear leaded transformation with corrected trend), Eq. (2), produces an excellent agreement between the 14C based TSI(S04) record of SSN, with a lead of 9400 yrs, with the model based on the temporal adjusted 10Be record, displayed in Fig. 3a. The corresponding TSI residue also has nonlinear recurrent oscillation, but with a period of ~1550 yrs. The nonlinear adjustment only required a change of sign in the first 1500 yr modeled. The residue of TSI, accompanied with its non-linear recurrent model, are displayed in **Fig. 3b**.

2.4 Application of the ~9500 yr recurrence of SA

We applied equation 3 with a lag parameter of 9600 yrs to the TSI records, maximizing the match between the analogue model based on S04 information and the original S04 records. Only the S04 model continually covers the next centuries, due to its longest characteristics, and presents an overlapping that explains 16% and 53.4% of the TSI variance of the last 1000 and 500 years, respectively. Results of TSI are displayed in Fig. 4. In this Figure, the three TSI records (S04, S09 and S12) are displayed with their analogue models.

1 However, in order to test the proposed method, we compare our TSI forecasts with a forecast
2 for the next 500 yrs based on S12 data and the Fast Fourier Transform (FFT) techniques
3 developed by S13. The TSI(S04) extrapolation explains 61.4% of the variance of the
4 forecasted TSI(S13) which is based on other data and other technique. This comparison
5 constitutes other important verifications and test of the proposed recurrent model of SA.

6 Our model confirms a Grand minimum in the period from 2050 to 2200 AD forecasted by
7 S13, characterized by showing a sustained deficit of 0.5 W/m², similar to that shown in the
8 Maunder Minimum, four centuries ago (see Fig. 4b).

9 The same model, shown in Figure 3a, suggests that the next Super-minimum of SA will occur
10 around 2100-2600 AD, and will be similar to the period 7500-7000 BP of reduced SA. In Fig.
11 3, big and small vertical orange arrows indicate Super and Grand solar minima, respectively.

12

13 2.5 Influences of the ~9500 yr recurrence of SA on continental tropical climate

14 Three models of the CTC temperatures, T_{crb}, based on different TSI reconstructions that
15 employed Eq. 2 are displayed in Figure 4. The modelling required a different modulation for
16 the first (M=2.) and second (M=1.) halves to distinctly consider the decreasing THC induced
17 deglaciation process until the stabilized Holocene periods (Piotrowski et al., 2004). These
18 models of T_{crb}, which were based on S04, S09 and S12 records, explain 30.0, 23.6 and 31.6
19 % and 6.5, 10.9, and 8.5 % of the reconstructed T_{crb} record for the periods from 20 to 10 and
20 from 10 to 0 Kyr BP, respectively. These three modelling results constitute other tests of our
21 recurrent model of SA. Note that the variance explanation is bigger in the first half of the
22 record when the THC was low and the

23 Finally, in another confirmation of not only the recurrent solar modelling, but their influences
24 on climate, we also apply equation 3 with a lag parameter of 9600 yrs to the CTC T_{crb} record.

25 Our model explains most of the variation of the T_{crb} during the past centuries. In a
26 comparison, partially depicted in Figure 5, the T_{crb} analogue model explains 7.3, 18.7, 60.8
27 and 71.7 % of the T_{crb} reconstructed record (W07) for the last 10, 5, 2 and 1 Kyr,
28 respectively. For the future, our model provides an estimation of a cooling for the 21st century
29 of about 0.5°C, followed by a slow warming trend with small oscillations during more than 4
30 centuries. The forecasts comparison also considers two different forecasts of TSI, shown in

1 Figure 3. With this comparison, we estimated that Tcrb analogue model also explains in the
2 2050-2500 AD period 34.3 and 37.1 % of variance of the TSI forecasts, based on S04 and S12
3 records (S13), respectively.

4 2.6 A model of the lagged response of the ECS

5 In Appendix C we present an analysis of the non-linear lagged responses of the Earth's
6 climate system (ECS). We propose and apply a power law to model Forcing Period-Response
7 Lag (P/L) relationships. Based on this power law, an estimation of the 1720+/- 400 yrs for the
8 response lag was made for the forcing period of ~9500 yrs. After its verification, we also
9 present, in Appendix C, an important example of the iron deposition in the south-western
10 Pacific [SWP] that lags solar activity by ~1500 yrs.

11 2.7 The lagged response of the sea level to solar recurrent forcing

12 In Appendix D, as an application and continuation of Appendix C, we present an analysis of
13 the lagged response of the sea level to CTC oscillatory forcing. We found that the sea level
14 lags the CTC signal by ~1500 yrs. Final results are displayed in Figure 7.

15

16 3 Discussion

17 Thanks to the recently developed paleoclimate records on solar-related and tropical climate
18 variability, we have found a ~9500 yr recurrence of SA and its linear influences on CTC.

19 Firstly, and in order to confirm this multi-millennial recurrence, we have developed different
20 tests and verifications of the SA and CTC recurrent patterns. In the following a summary of
21 the tests and verifications of our findings is presented:

22 A. Our FS model explains the detrended and modulated 10Be statistically corrected
23 variability over almost the last 40 Kyr. However the recurrent patterns based on
24 FN97 when extrapolated backward in time are comparable with independent 10Be
25 information from the Eemian.

26 B. When this recurrent phenomena detected in the 10Be record was extrapolated to the
27 TSI records, we conducted other tests, establishing the following: a) the overlapping
28 of the TSI(S04) record explains over 53% of the variance in the last five centuries; b)
29 the extrapolated model also based on TSI(S04) presents an important match with

1 different data (S12) and an independent procedure (FFT) employed in the TSI forecast
2 due to S13; and c) the extrapolated models [TSI(S04), TSI(S09), and TSI(S12)], but
3 backward in time (See Fig. 5), present an important match with independent CTC
4 Tcrb (W07).

5 C. When this recurrent phenomena detected in the 10Be record was also extrapolated to
6 the CTC Tcrb record, we conducted another test, establishing that: a) the overlapping
7 of the Tcrb (W07) record explains over 71% of the variance in the last millennium;
8 and b) the analogue model extrapolated forward in time presents an important match
9 with, based on different data (S12) and an independent procedure (FFT) employed in,
10 the TSI forecast due to S13.

11 D. In Appendix B, we developed an empirical analysis of the solar gravitational forcing
12 due to lateral forces. There we found that lateral forces generate a low-frequency
13 signal, preceding by ~6700 yrs low-frequency solar activity. This lag appears to be
14 part of the non-linear lagged responses of solar activity to different time-length
15 gravitational forcing. This lateral forcing could enhance the oblateness of the solar
16 body, and consequently the tidal influences on the sun. In the same Appendix B, we
17 also verify that: a) the solar patterns of 9600 and 10.5 yrs are similar, suggesting a
18 common gravitational origin, and b) the patterns of lateral force show similarities in
19 solar activity in different scales

20 E. The qualitative verification of the total solar irradiance (TSI) ~9.5Ky recurrent
21 patterns with a bivalve population (BVpop) reconstructed from late Miocene
22 (~10.5Mya) data, shown in Appendix A, confirms not only the geological existence of
23 this recurrent solar pattern, but also its period because the comparison is made with
24 the extrapolated forward in time records (see Appendix A and Fig. 4).

25 Our experimental multi-millennial-scale analogue forecast of TSI, supported mainly by
26 recurrent oscillations over the last glacial-interglacial cycle, shows a lowering trend toward a
27 minimum for the coming decades. Our forecast also confirms previous efforts by several
28 authors (Fairbridge and Sanders, 1987; Fairbridge and Shirley, 1987; Perry and Hsu, 2000;
29 Duhau and Jager, 2010), who have forecasted a solar Grand Minimum for the upcoming
30 decades. For instance, recent findings linked to periodicities of the solar tachocline and their
31 physical interpretation may permit us to estimate that solar variability is presently entering

1 into a long Grand Minimum, thus consisting of an episode of very low SA (Duhau and Jager,
2 2010).

3 Although the complete physical basis of this recurrent process is missing, there are several
4 examples of physical and theoretical evidence that also support our findings. Firstly, it is
5 important to highlight what Mackey (2007) has stated: “In several papers, Rhodes Fairbridge
6 and co-authors described how the turning power of planets is strengthened or weakened by
7 resonant effects between the planets, the sun and the sun’s rotation about its axis.”

8 Specifically, there are important works motivated by Rhodes Fairbridge and other researchers,
9 providing a theoretical basis and practical evidences of resonant interactions, for instance:

10 A. Abreu et al. (2012) have shown the physical basis of a gravitational forcing of the
11 solar tachocline variations. They developed a gravitational model for describing the
12 time-dependent torque exerted by the planets on a non-spherical tachocline and
13 compared the corresponding power spectrum with the reconstructed SA record. They
14 find an excellent agreement between the long-term cycles in proxies of SA and the
15 periodicities in the planetary torque (with a period from 50 to 504 yr).

16 B. Fairbridge and Sanders (1987) have indicated long-term variations due to planetary
17 forcings. They follow Stacey (1963) who, based on the periodicities of planetary
18 orbits, proposed a ~4.45 Kyr Outer Planets Restart (OPR) cycle. It is close to half of
19 the ~9.5 Kyr detected periodic recurrence.

20 C. Focused on Moon-Earth gravitational links, Keeling and Whorf (2000), based only on
21 the links expressed in tidal astronomical periodicities, have proposed a ~1.8 Kyr that
22 represents the time for the recurrence of perigeon eclipses closely matched with the
23 time of perihelion. This cycle is near the fifth part of the ~9.5 Kyr detected periodic
24 recurrence. Keeling and Whorf (2000) also detected in their analysis a ~4.65 Kyr
25 modulation cycle of the 1.8 Kyr that is almost half of the ~9.5 Kyr detected periodic
26 recurrence.

27 D. Looking for solar-planetary resonances of our detected ~9.5 Kyr, we compared the
28 “biggest” solar system secular frequencies determined by Laskar (2011) over 20 Ma
29 for the four inner planets, and over 50 Ma for the five outer planets, corresponding to
30 45.184 and 49.880 Kyr, respectively. We found that the mean value of 47.532 Kyr is
31 almost five times the solar period detected ($47.532 \text{ Kyr} = 5 \times [9.56 \text{ Kyr}]$). This means

1 that the solar inner and outer planets show a resonance (5:1) with the solar periodicity
2 detected.

3 E. We also compared the equatorial insolation variability recently evaluated by Berger et
4 al. (2006), who, in line with Milankovitch ideas on astronomical forcing, evaluate,
5 using astronomical models and the MTM spectral techniques, significant 95 Kyr and
6 123 Kyr periods related to eccentricity periods. The lowest value of 95,000 yrs is
7 almost ten times the solar period detected. This also means that one of Earth's primary
8 eccentricity periods is in resonance (10:1) with the solar periodicity detected.

9 We have found and tested a recurrence of ~9500 yrs of SA that implies a solar Grand-
10 minimum for the next one and a half centuries. However, we can also support our findings
11 with other studies. For instance, the existence of different solar modes of activity (Grand
12 minima, Regular, and a possible Grand maxima), which have also shown important temporal
13 variations with asymmetries (Grand maxima significantly less often experienced than Grand
14 minima) during the Holocene (Usoskin et al., 2014), would be considered expressions of our
15 detected recurrent pattern of ~9500yrs.

16 In this work, we have forecasted a continuation of the solar decline for the next decades,
17 which is supported through precursory signals during recent decades:

18 a) A steady and systematic decline in solar polar magnetic fields, starting from
19 around 1995, which is well correlated with changes in meridional-flow speeds
20 (Janardhan P., Bisoi, S. K., Gosain S., 2010)

21 b) A decline in solar wind micro-turbulence levels. Based on extensive interplanetary
22 scintillation (IPS) observations at 327 MHz, obtained between 1983 and 2009, a
23 steady and significant drop in the turbulence levels in the entire inner heliosphere,
24 starting from around ~1995, was detected (Janardhan et al., 2011).

25 c) A significant reduced ionospheric cut-off frequency to radio waves, normally
26 about 30 MHz, to well below 10 MHz (Janardhan et al., 2015a).

27 Also, in this work, we have forecasted a Grand solar-minimum, with sustained low solar
28 activity for the next two centuries, which has been supported through a number of recent
29 studies and their findings:

1 a) The continuation of this decline in solar activity is estimated to continue until at
2 least 2020, and there is a good possibility of the onset of a Grand solar minimum
3 from solar-cycle 26 onwards (2031) (Janardhan et al., 2015b).

4 b) Based on the S04 SA record, it has been shown that gradual (abrupt) changes in
5 solar surface meridional flow velocity lead to a gradual (abrupt) onset of grand
6 minima, and that one or two solar cycles before the onset of grand minima, the
7 cycle period tends to become longer (Choudhuri and Karak, 2012; Karak and
8 Choudhuri. 2011). It is noteworthy that surface meridional flows over Cycle 23
9 (Hathaway and Rightmire, 2010) have shown gradual variations, and Cycle 24
10 started 1.3 years later than expected.

11 ~~Finally, we would like to emphasize the social importance of these multi-millennial solar~~
12 ~~oscillations is clearly shown if we consider that the world population began an almost~~
13 ~~sustained exponential increase was a lagged response to the past solar Super-minimum at~~
14 ~~~7000-yr BP, when a multimillennial period of increasing solar activity provided favorable~~
15 ~~environments for developing the first civilizations all around the world (REF+++++). Also,~~
16 ~~in that work a detailed analysis about the detection and empirical modelling of solar and~~
17 ~~terrestrial variability of ~2400-yr recurrent patterns and its potential influences on the world~~
18 ~~population over past and future millennia is presented and discussed.~~

19 The detected modulation of CTC Tcrb record, occurring during the interglacial could be
20 linked to the increasing THC that has been reconstructed by Piotrowski et al. (2004):
21 “Neodymium isotope ratios in the authigenic ferromanganese oxide component in a
22 southeastern Atlantic core reveal a history of the global overturning circulation intensity
23 through the last deglaciation...It exhibits a gradually increasing baseline intensity that
24 plateaus in the early Holocene.”

25 This increasing THC implies greater oceanic heat transport from the tropics and a consequent
26 lower thermal response of the CTC. About sudden climate changes during the interglacial,
27 Clarke et al, (2001) have pointed out: “Studies of deep ocean sediments and ice cores as well
28 as coupled climate model simulations have identified changes in the THC in the North
29 Atlantic as the probable mechanism. The warm events are though to have occurred when the
30 THC penetrated further into the Nordic sea, whereas the cold events coincided with times at
31 which the THC has slackened, reducing the transport of warm water to the North Atlantic.”

1 Also, we have found a common process of the historically detected lags in different climate
2 scales and processes.

3 The existence of thermal, rheological and mechanical inertias caused by ice-melting and
4 thermo-haline circulation (THC) processes shows a common non-linear, power law model.
5 See more discussion in Appendix C.

6 In Appendix D we have also presented an analysis of climate lags, focused on one of the most
7 representative variables, the sea level, which presents important lags in different scales. In this
8 Appendix, a lagged (~1550 yrs) sea level (SL) response assessed for the last 12 Kyr, and
9 extrapolated for the next millennia, was associated with the detected solar oscillation of
10 ~9500 yrs. See Figure 7 and more discussion in Appendix D.

11 **4 Conclusions**

12 An analysis and test of recurrent solar variability for the last millennia has been presented in
13 this study. It was based on five multi-millennia solar-related reconstructed records from
14 different and valuable proxy information.

15 The tested existence of the ~9.5 Kyr period recurrent pattern suggests that SA is characterized
16 by solar dynamics with long-term patterns. Considering that it has been suggested that the
17 modulating oscillations of SA, around 84, 178 and 2400 years, are possibly related to the
18 Sun's rotation rate and impulses of the torque in the Sun's irregular motion (Landscheidt,
19 1999; Fairbridge and Sanders, 1987; Charvátová, 1995; Charvátová, 2000), our results also
20 suggest that similar mechanisms on the solar dynamo must be proposed for solar oscillations
21 of around 9.5 Kyr. This hypothesis should be tested, taking into account the results presented
22 in this paper.

23 In this direction, we present two evidences of the solar recurrent pattern. In Appendix A, we
24 present a qualitative verification of the total solar irradiance (TSI) ~9.5Ky recurrent patterns
25 with a bivalve population (BVpop) reconstructed from late Miocene (~10.5Mya) data that
26 shows the persistence and regularities of the solar patterns.

27 In Appendix B, we present an empirical analysis of solar gravitational forcing due to lateral
28 forces. We found that lateral forces generate a low-frequency (~9500 yr) signal that presents
29 similarity with, and precedes by ~6700 yrs, low-frequency solar activity. This lateral forcing
30 could enhance the oblateness of the solar body, and tidal influences, and consequently, as
31 Abreu et al. (2012) have also suggested, regular cycles of solar activity.

1 With all of these recurrent phenomena, we have presented, tested and verified an experimental
2 multi-millennial forecast technique for SA. We have provided elements and supporting recent
3 studies on precursor signals of an entering into a Grand minimum SA mode. The extreme
4 duration of the last solar minimum, is important evidence of longer cycles, similar to those
5 presented before the start of the Maunder and Sporer minimum.

6 The response of the ECS to solar forcing variability of ~9500 yrs is demonstrated in
7 Appendixes C and D, associated with a lagged response of ~1550 yrs for both the sea level
8 and geochemistry of the ocean. In particular, we have proposed, applied, and verified a
9 simple power law model of the lagged response of the ECS to different forcing phenomena
10 during geological, orbital and suborbital time-scales.

11 The consequent forecasted trend toward these Grand (Super)-minima of TSI conditions is
12 very important from a paleoclimatic perspective, because information from different
13 reconstructions and models indicates a potential **continental** tropical temperature cooling of
14 around 0.5°C for the rest of the 21st century, a warming of around 0.65°C from the end of the
15 21st century to the end of the 23th century, a cooling of around 0.3°C from the end of the 23rd
16 century to the middle of the 23th century, and a warming of around 0.65°C from the middle of
17 the 23rd century to the end of the 25th century without taking into account volcanic and
18 anthropogenic forcing.

19 The recurrence in solar activity was verified through its influence on CTC. Three models of
20 the CTC temperatures, T_{crb}, based on different SA reconstructions were evaluated. The
21 modelling required a different modulation considering the increasing THC process. These
22 three modelling results constitute other tests of our recurrent model of SA.

23 The assessed connection between TSI and CTC is also supported by previous studies, such as
24 those by Berger et al. (2006), who pointed out that “the equatorial and inter-tropical regions
25 can play an important role in the response of the climate system to the astronomical forcing.”

26 The modulated connection between TSI and CTC helps us to confirm the previous studies on
27 THC, such as those by Piotrowski et al. (2004), who pointed out that “The gradually
28 increasing baseline through the deglaciation indicates that THC does not switch between
29 distinct glacial and interglacial modes of circulation but rather that varies as a continuum.”

30 However, more research is needed to better understand the solar recurrent patterns and their
31 influences not only in the tropical climate but also in the global climate, because, as Peeters et

1 al. (2004) have suggested, the Mozambique and Agulhas currents in the western Indian Ocean
2 could be an efficient carrier of the CTC signal (influenced by SA) to the global scale.

3 It has been demonstrated with a decreasing sea level trend for the next millennia, forecasted
4 and verified in Appendix D, as a natural lagged (~1550 yrs) response of our ECS to the
5 recurrent solar signal of ~9500 yrs.

6 Our final remarks are the following:

7 A. The detected lagged response of the ECS will be useful for proposing internal and/or
8 external forcing mechanisms in future modeling efforts on multi-decadal and longer
9 time scales.

10 B. Our results also support that lagged responses are required for accurate modeling and
11 forecasting of climate-related issues. However, further multi-disciplinary scrutiny and
12 modeling efforts are still required.

13 C. Our results have placed natural climate variability in an important place for climate
14 modeling and analysis, and of course, for climate forecasting. Also, our results have
15 clearly shown how important Holocene climate events would be better understood
16 with climate reconstructions, analysis and recurrences.

17 D. The forecasted trends and minima are of great interest not only for the solar and
18 terrestrial climate, but also for socio-economic planning, since climate variability has
19 led to important impacts in different economic and social sectors of our societies
20 around the world.

21 E. Our findings strongly suggest that recurrent variability may play an active role in
22 natural climate change during the coming decades, centuries and millennia.

1 Appendix A: Qualitative verification of total solar irradiance (TSI) ~9.5Ky
2 recurrent patterns with a bivalve population (BVpop) reconstructed from late
3 Miocene (~10.5Mya) data

4

5 In a recent paper Harzhauser et al. (2013; H13 hereafter) analyze the explosive demographic
6 expansion by dreissenid bivalves as a possible result of astronomical forcing. These authors:
7 a) reconstruct the extinct bivalve species *Sinucongeria primiformis* in a lacustrine system of
8 Lake Pannon during the Tortonian (~10.5 Mya; late Miocene), with 600 samples that cover
9 about eight millennia of late Miocene time with a decadal resolution; and b) detect bivalve
10 population regular fluctuations possibly linked to solar activity. H13 have pointed out: “Our
11 data indicate that the settlement by bivalves in the off-shore environment was limited mainly
12 by bottom water oxygenation, which follows predictable and repetitive patterns through time.
13 These population fluctuations might be related to solar cycles: successful dreissenid
14 settlement is recurring in a frequency known as the lower and upper Gleissberg cycles with
15 50–80 and 90–120 yr periods. These cycles appear to control regional wind patterns, which
16 are directly linked to water mixing of the lake. This is modulated by the even more prominent
17 500 yr cycle, which seems to be the most important pacemaker for Lake Pannon hydrology.”

18

19 In this comment, we extend the H13 detected solar-terrestrial connections (TSI-BVpop) to the
20 complete reconstructed ~8Kyr BV record, comparing the reconstructed record with the
21 average of the S04, S09 and S12 TSI records extrapolated forward in time (Fig 4.).

22

23 An initial comparison, shown in Figure A.1, demonstrates the existence of millennia and
24 multi-millennia scale oscillation in TSI and BV series of anomalies. However, when an
25 adjustment (a linear transformation) and a lower threshold for TSI are applied, the following
26 comparison, shown in Figure A.2, better demonstrates the existence of millennia and multi-
27 millennia-scale similar oscillation in TSI and BVpop series of anomalies.

28

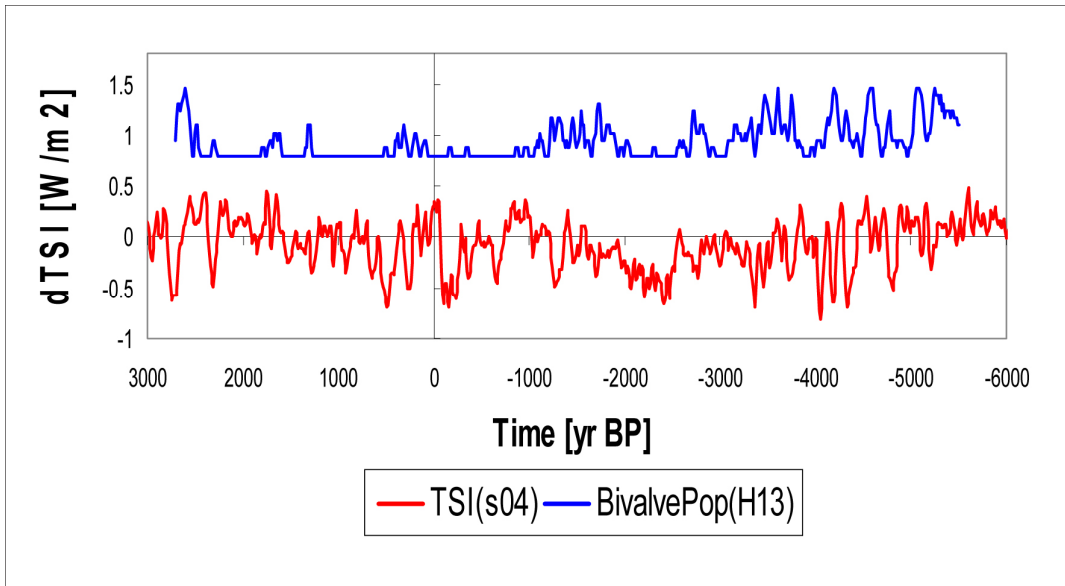
1 This simple trend adjustment of the TSI could be justified by the orbital phenomena of
2 eccentricity and obliquity that can modulate solar influences in periods of 100 and 40 Kyr,
3 respectively. Additional adjustments in the BVpop timing could improve the match.

4

5 REFERENCES

6

7 Harzhauser, M., Mandic, O., Kern, A.K., Piller, W.E., Neubauer, T.A., Albrecht, C., Wilke,
8 T. 2013. Explosive demographic expansion by dreissenid bivalves as a possible result of
9 astronomical forcing. *Biogeosciences*, 10, 8423-8431.



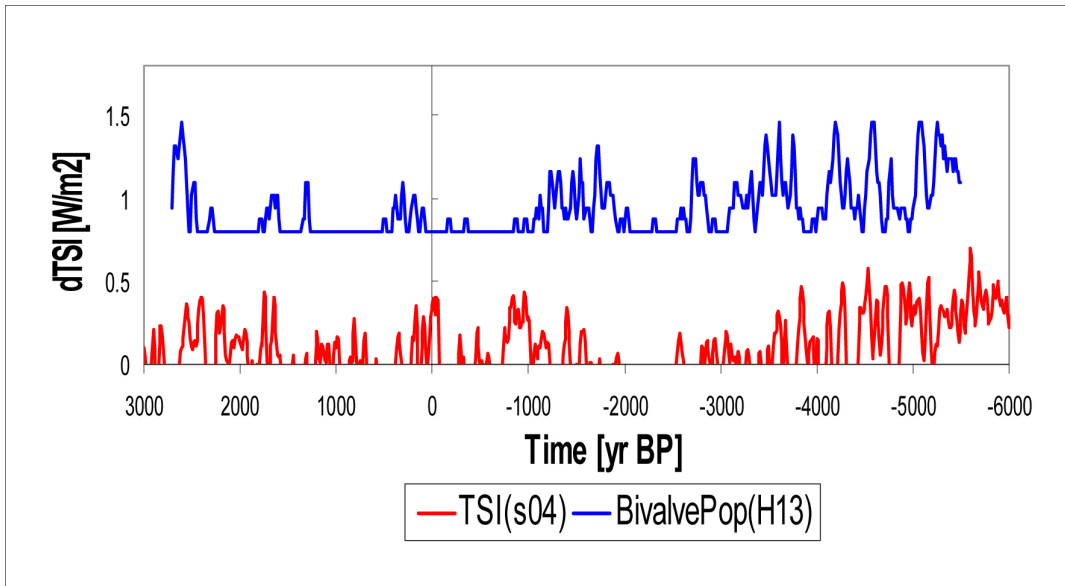
1

2

3

4

Figure A.1. Comparison of bivalve population (BVpop) and TSI. A linear transformation [BVpop(H13)=aBVpop(H13)+b] with a factor a=0.22 and a bias b=0.8.



1
2
3
4
5
6
7

Figure A.2. Comparison of bivalve population (BVpop) and TSI adjusted with a linear transformation $[TSI_{adj} = TSI + a(t-t_1) + b]$ with $a = .03 [W/m^2]/1000[yr]$ and $b = -0.3 [W/m^2]$.

Only positive TSI adjusted anomalies are displayed in order to enhance the match and show a possible threshold provided by TSI for BVpop development.

1 Appendix B: Empirical evidence of a planetary gravitational forcing of the
2 ~9500yr total solar irradiance (TSI) recurrent pattern

3

4 Planetary gravitational forcing (PGF) of solar activity (SA) has been considered by many
5 solar researchers (see references in the main part). However, numerical simulations of this
6 forcing have been analyzed by only a few of them. For instance, Abreu et al. (2012) analyzed
7 the PGF of solar tides. In this comment, we compare the lateral (perpendicular to movement)
8 forces evaluated by lateral accelerations of the solar movement around the solar system (SS)
9 barycenter (BC) with TSI reconstructed and extrapolated (based on the detected recurrences)
10 records. Our work is motivated by the findings from Fairbridge and Shirley (1987), who
11 predicted the initiation of a Maunder-type prolonged minimum on the basis of a study of solar
12 motion with respect to the SS-BC in the years from 760 to 2100 AD. Their study detected
13 “patterns” in solar orbits associated with different levels of SA.

14

15 In order to analyze variability in both solar dynamics and solar activity, we studied data
16 coming from: a) lateral forces (F) of the sun due to planetary gravitational forces and
17 movements, reconstructed and forecasted by JPL/NASA from 3000 BC to 3000 AD, and b)
18 solar activity expressed in the total solar irradiance (TSI) average from three reconstructed
19 records over the last millennia and extrapolated for the next millennia (all shown in Figures
20 3a). These two records are displayed in Figure B.1.

21

22 Lateral (perpendicular to movement) forces were evaluated based on X, Y and Z coordinates
23 and derivatives provided by the HORIZONS (H) system from the Jet Propulsion
24 Laboratory/NASA (JPL/NASA) for the past 5000 and future 1000 years, every 90 days,
25 where the XY plane is the ecliptic plane centered on the BC. As an approximation, solar
26 movement was considered only in the XY plane, and lateral acceleration in this plane was
27 evaluated to be perpendicular to the tangential direction of solar movement. These on-line
28 solar system data and ephemeris computation services provide accurate ephemerides for solar
29 system objects.

30

1 The simulated lateral inertial forces (F) are considered to provide gravitational influences on
 2 solar activity. In order to enhance their low-frequency oscillations, we applied the double
 3 integral function to the analyzed F record.

4

5 An integration was applied twice to the Solar signal, $S(t)$, as follows:

6

$$7 \quad \sigma S_1(t) = \int_{t_0}^t (S(t) - \mu_S) dt \quad (B1a)$$

$$8 \quad \sigma S_2(t) = \int_{t_0}^t (\sigma S_1(t) - \mu_{S_1}) dt \quad (B1b)$$

9 Where, $S(t)$ is the solar signal, expressed as force ($F(t)$) or total irradiance ($T(t)$), t is time, t_0 is
 10 initial time, $\sigma S_N(t)$ is its time integral, N is the successive application number, and μ_S and
 11 μ_{S_1} are the long-term averages of $S(t)$ and $\sigma S_1(t)$, respectively.

12

13 We apply equations B1a and B1b to these two records in order to enhance low-frequency
 14 variations. Results are displayed in Figure B.2. The double integral of forces F , $\sigma F_2(t)$, is
 15 almost explained (99.9 % of variance) by a sine function of a 9400 yr oscillation, which is
 16 also displayed in Fig. B.2a. The double integrated solar activity TSI, $\sigma T_2(t)$, also shows a
 17 periodicity of ~9500 yrs. The scales of these enhanced solar signals are inverted because the
 18 sign is changed due to the double integration enhancement. A comparison of both curves is
 19 displayed in Figure B.3a. Figure B.3b also displays both integrated curves, however the
 20 $\sigma T_2(t)$ curve is leaded (moved backward in time) 6700 yrs.

21

22 In order to verify this 6700 yr lag of the TSI response to the F oscillation of a 9500 yr period,
 23 we look for two other similar pairs of periods and lags (P/L). In order to obtain an additional
 24 pair of P/L, we analyze the lateral force F and solar activity TSI over the 1000-3000 AD
 25 period. We applied a double integration (Eq. B1) and a polynomial detrending process to F.
 26 The $\sigma T_2(t)$ and its trend is shown in Figure B.4. The detrended $\sigma T_2(t)$ is compared with the
 27 TSI record, and oscillations of ~950 yrs are detected, together with a lag of ~350 yrs of TSI
 28 with respect to the supposed forcing F. These two variables are displayed in Figure B.5.

29

30 Another pair of P/L values is evaluated with the Hale SSN cycle of ~22 years that shows an
 31 alternating magnetic sign for each 22 yrs. It is compared with the Fourier series (with only 2
 32 harmonics) of the force F, signal based on the period from 1700 to 2000 AD. The comparison,
 33 depicted in Figure B.6, indicates a lag of less than 1 year.

1

2 The three sets of L/P pairs are 1/22, 350/950 and 6700/9500 yrs, respectively. These three
3 pairs, which correspond to different phases, are modeled together with a non-linear function
4 that tends toward a lower limit of 0° for lower periods, and an upper asymptotic limit of 360°
5 (2π radians). The adjusted model for phase variations in terms of period, which is a
6 logarithmic function, is depicted in Figure B.7.

7

8 It is important to emphasize that the results in Figure B.5 have not only detected an L/P pair
9 but also confirm the next forecasted Grand Minima (2020-2220 AD) also associated with
10 contributions from unexplained modulation process of ~ 350 -yr-lagged-influences of solar
11 lateral forces.

12

13 Additionally, we developed an interesting comparison that shows self-similarity in TSI.

14 This comparison is for our enhanced $\sigma T_2(t) \sim 9500$ -yr-solar-cycle, evaluated previously, with a
15 Fourier series model of the solar SSN cycle with a period of 10.5yrs, based on monthly SSN
16 data from the World Data Center SILSO, Royal Observatory of Belgium, Brussels, over the
17 period from 1964 to 2008. This comparison is displayed in Figure B.8, and clearly shows self-
18 similarities between these two solar cycles. Both cycles show a shorter increasing period
19 ($\sim 25\%$) than the decreasing period ($\sim 45\%$), and a maximum plateau ($\sim 20\%$), and an almost
20 nonexistent minimum plateau.

21

22 Finally, we also developed a spectral analysis of the analyzed lateral forces. This analysis is
23 based on wavelets and is displayed in Figure B.9. It clearly shows important contributions to
24 periods around of 8, 22, 60 (in a range of 50-80), 180, 650 (in a range of 400-800), 1000 and
25 2500 years.

26 Based on both a) the SS movement reconstruction and simulation, H services, developed by
27 the Solar System Dynamics Group of the JPL/NASA, and b) monthly SSN data from the
28 World Data Center SILSO for the last decades, we have provided additional elements to
29 support the idea that long-term solar activity is modulated by recurrent planetary effects. Our
30 analysis has put forward the following:

1

2 1) SS dynamics generate lateral forces (enhanced by $\sigma F_2(t)$) with multi-millennia scale
3 (~9500 yr) oscillations similar to those shown by solar activity (enhanced by $\sigma T_2(t)$);

4 2) There is a suggested lagged response of around 67 centuries, of solar activity ($\sigma T_2(t)$) to
5 the gravitational forcing (lateral force). The maximum forces F precede the maximum solar
6 activity TSI, meaning that increases (decreases) of force F produce lagged increases
7 (decreases) of TSI;

8 3) Taking into account that the Sun's rotation axis is tilted by about 7.25 degrees from the axis
9 of the Earth's orbit, the PGF are able to generate meridional forces and consequently
10 meridional circulations in the Sun;

11 4) The lagged response appears to increase with forcing periods with a non-linear logarithmic
12 function that implies temporal scale influences and possible connections with meridional
13 circulations in different deep layers of the Sun;

14 5) The similarity of the ~9500yr TSI with the average SSN 10.5yr cycle, with scales differing
15 at almost three orders of magnitude, suggests a self-similar process with a mechanism
16 possibly linked to recurrent PGF in different scales.

17

18 REFERENCES

19

20 HORIZONS System. Documentation of JPL Horizons (Version 3.75)
21 Apr 04, 2013. ftp://ssd.jpl.nasa.gov/pub/ssd/Horizons_doc.pdf. [Data retrieved at:
22 www.ssd.jpl.nasa.gov/?horizons]

23

24 Abreu, J. A., Beer, J., Ferriz-Mas, A., McCracken, K. G., Steinhilber, F., 2012. Is there a
25 planetary influence on solar activity? *Astronomy & Astrophysics*, 548, A88 (2012)

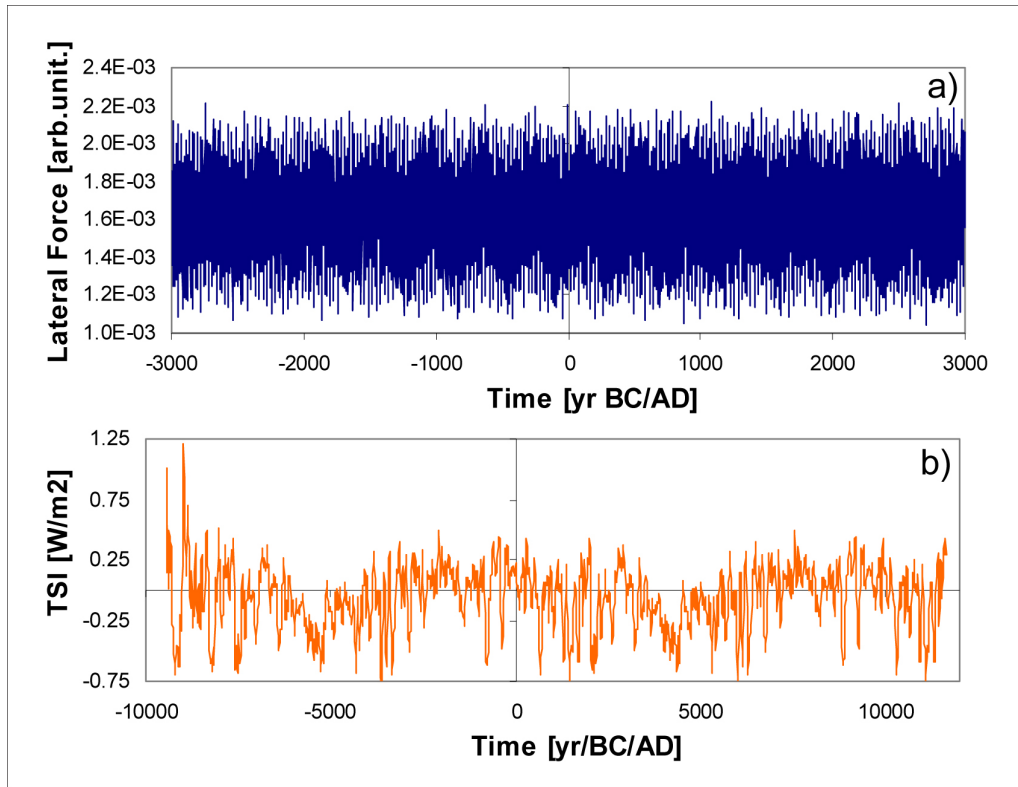
26 DOI: 10.1051/0004-6361/201219997

27

1 SILSO, World Data Center - Sunspot Number and Long-term Solar Observations, Royal
2 Observatory of Belgium, on-line Sunspot Number catalogue: [Data retrieved at:
3 <http://www.sidc.be/silso/datafiles>].

4

5



1

2

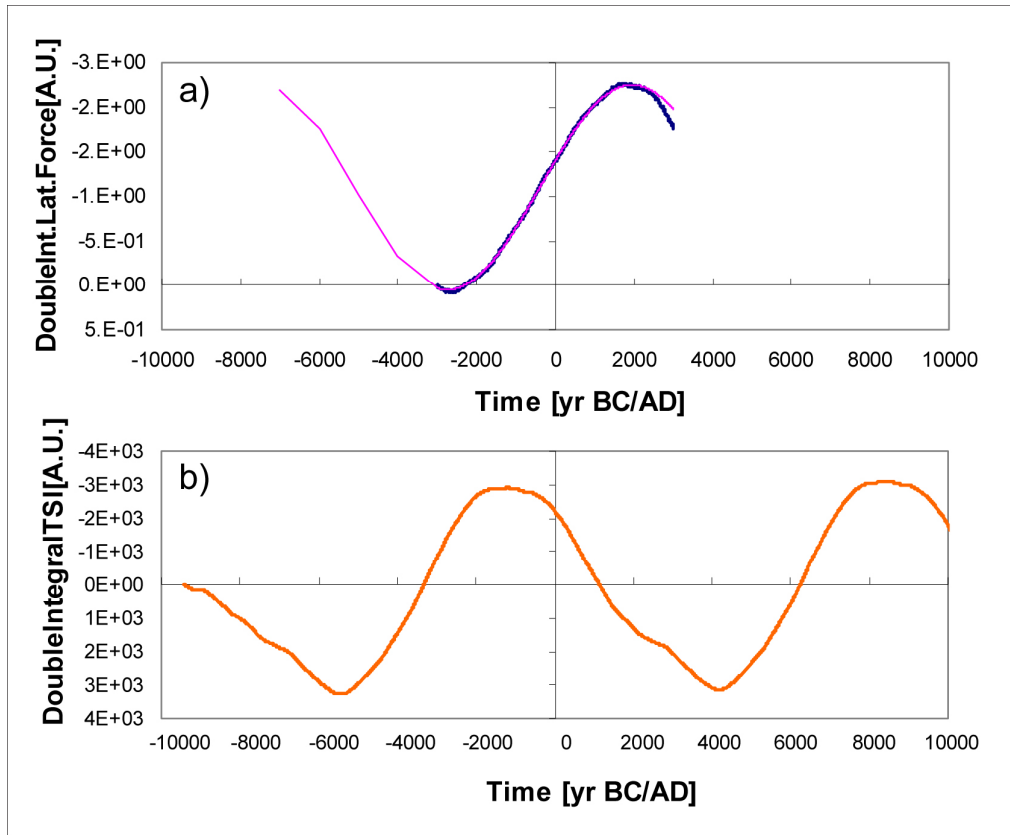
3

4

5

6

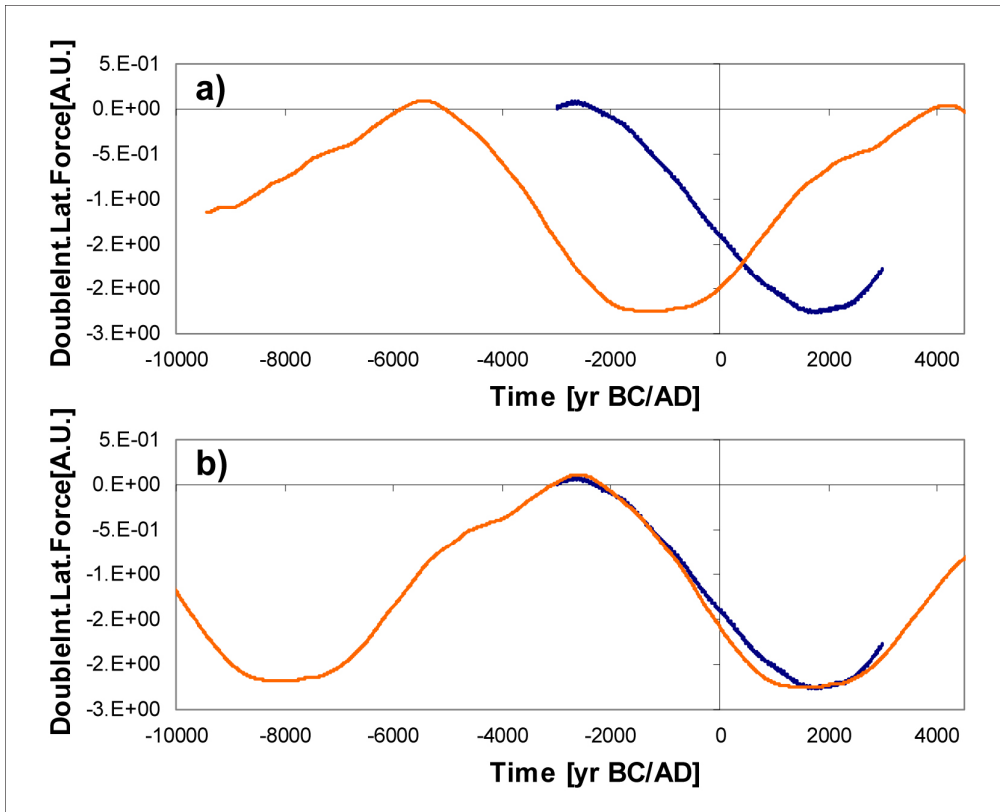
Figure B.1. a) Lateral forces on the Sun generated by planetary gravitational forces (PGF), expressed in [arbitrary units], evaluated by the Horizon/NASA system from 3000 BC to 3000 AD. b) The solar activity (TSI) expressed in [W/m²], average values of the three reconstructed records over the last millennia and extrapolated for the next millennia (10000 BC to 10000 AD) based on ~9500 yr recurrence (records shown in Figure 3a).



1

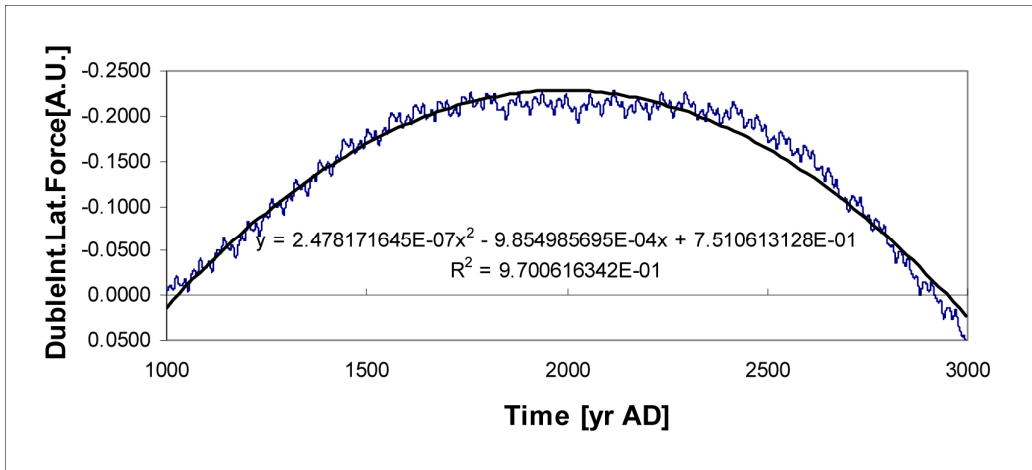
2

3 Figure B.2. a) Double integral of the solar lateral inertial forces $\sigma F_2(t)$ due to the solar movement resulting
 4 from the planetary gravitational forces shown in Figure B.1.1a, and b) Double integral of the solar reconstructed
 5 and extrapolated record $\sigma T_2(t)$ shown in Figure B.1.1b. Vertical scale of values were inverted both in
 6 $\sigma F_2(t)$ and $\sigma T_2(t)$ because the double integral procedure changes the sign of the enhanced result. Please note
 7 that the last minimum of lateral inertial force F was around 2500 BC and the next minimum of TSI will be
 8 expected around 4200 AD.



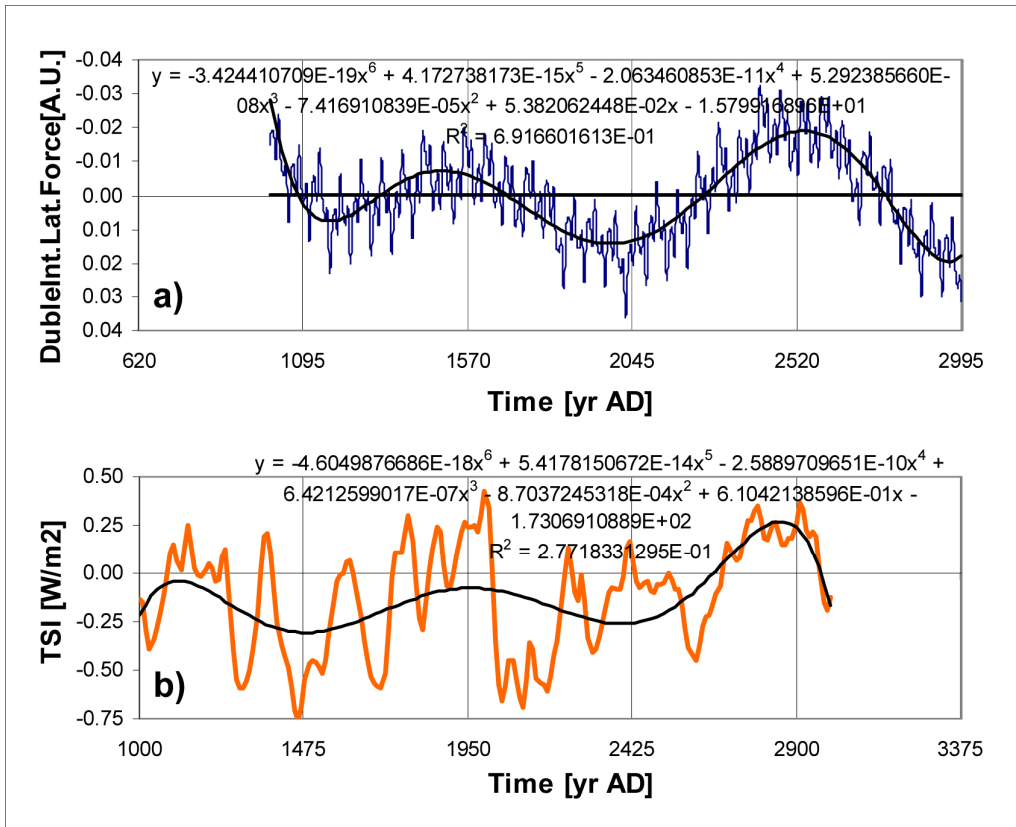
1
2
3
4
5
6
7

Figure B.3. A comparison of the double integral of the solar lateral inertial forces $\sigma F_2(t)$ and the solar reconstructed and extrapolated record $\sigma T_2(t)$. To enhance a possible cause-effect relationship [$\sigma F_2(t)$ - $\sigma T_2(t)$] the $\sigma T_2(t)$ record is shown a) without and b) with a lead of 6700yrs.



1
2

3 Figure B.4. The double integral of the solar lateral inertial forces $\sigma F_2(t)$ for the period from 1000 to 3000 AD.
4 A polynomial trend is also depicted.



1

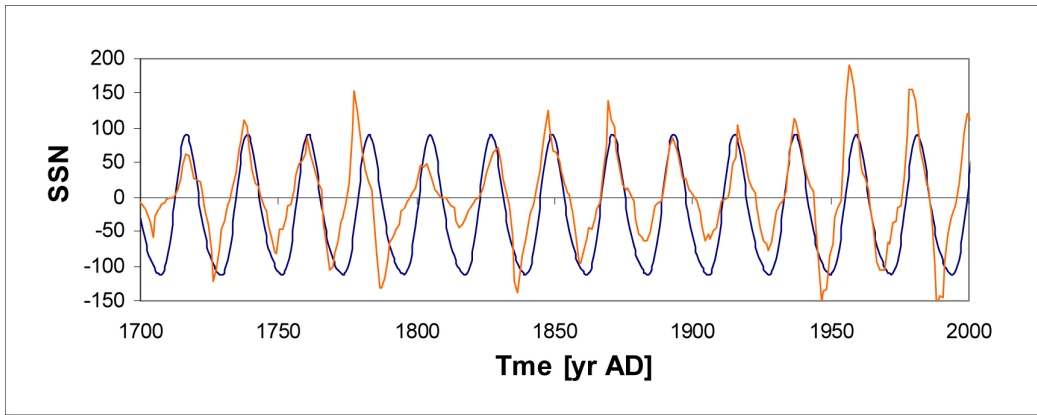
2

3

Figure B.5. A comparison of the double integral of the solar lateral inertial forces $\sigma F_2(t)$ and the solar reconstructed and extrapolated record TSI. To enhance trends, polynomials are adjusted to both records, showing oscillations of ~950 yrs and a lag of ~350 yrs.

4

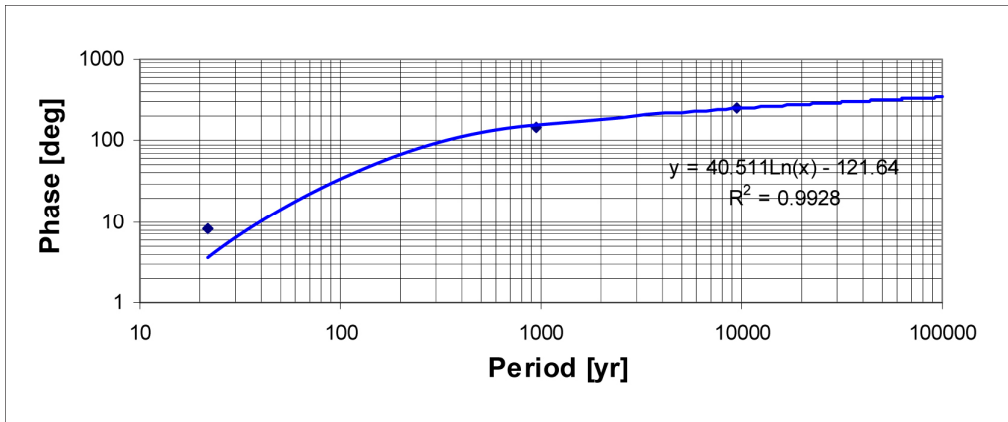
5



1

2

3 Figure B.6. A comparison of the Hale solar cycle of SSN and the Fourier Series (with only 2 harmonics) model
4 of the F signal. A lead of 0.5 yrs is applied to the SSN to improve the match with the F recurrent model.



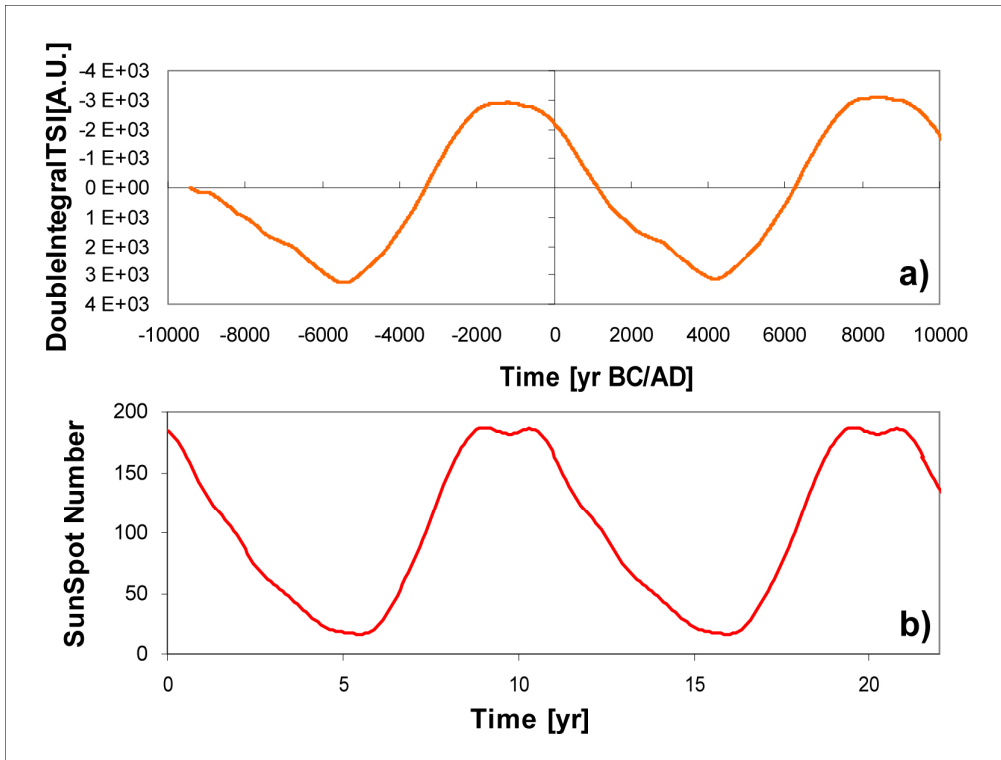
1

2

3 Figure B.7. A model of phase between F (forcing) and TSI (suggested response) signals for different periods.

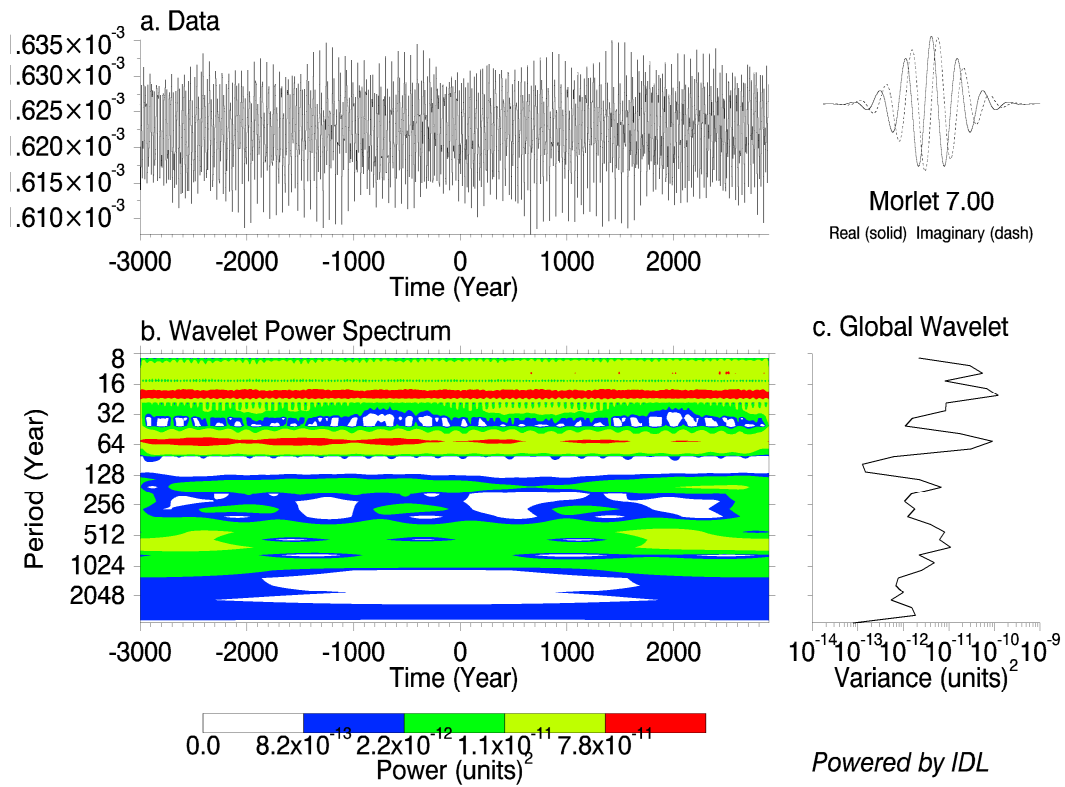
4 The adjusted logarithmic model, which explains 99.5 % of the variance, shows two trends, one to zero for short

5 periods, and other, an asymptotic one, for long periods.



1
2
3
4
5
6
7
8

Figure B.8. Comparison of: a) the double integral of the reconstructed solar activity (TSI), and b) the mean solar cycle obtained with a FS model based on SSN data from the World Data Center SILSO, Royal Observatory of Belgium, Brussels, over the period from 1964 to 2008.



1

2 Figure B.9. (a) Lateral Force [arbitrary units]. (b) The wavelet power spectrum. The contour levels are chosen so
 3 that 75%, 50%, 25%, and 5% of the wavelet power is above each level, respectively. The cross-hatched region is
 4 the cone of influence, where zero padding has reduced the variance. (c) The global wavelet power spectrum
 5 (black line). The dashed line is the significance for the global wavelet spectrum, assuming the same significance
 6 level and background spectrum as in (b). Reference: Torrence, C. and G. P. Compo, 1998: A Practical Guide to
 7 Wavelet Analysis. Bull. Amer. Meteor. Soc., 79, 61-78.

1 Appendix C: Non-linear lagged responses of the Earth's climate system (ECS):

2 A power law, its verification, and an example (Iron deposition in the south-
3 western Pacific lags solar activity by ~1500 yrs)

4
5 Climate & Sea-level (C&SL) responses to different climate forcing (CF) variability, over the
6 Phanerozoic and the last glacial-interglacial cycles, are jointly analyzed based on previous
7 studies of C&SL reconstructed records. Our analysis suggests that C&SL responses are forced
8 by different processes with different lagged responses through mechanisms possibly
9 associated with the crustal movements and thermohaline currents that move mass (soil, water
10 and salt) and energy against the thermal-rheological-mechanical (TRM) inertias of continents,
11 oceans, glaciers and ice-sheets. The non-linear response appears to be frequency dependent
12 and is verified twice, based on published data of multi-annual and centennial SL lagged
13 responses. Our power law model suggests, for the ~9500 yr detected solar oscillation, a
14 millennial-scale climate lagged response, which is verified with an oceanographic record of
15 iron deposition in the south-western Pacific [SWP] that lags ~1500 yrs solar activity.

16
17 ***The Earth's climate (and sea level) lagged response***

18 It should be mentioned, first of all, that sea level is affected by plate collisions. For instance,
19 the crustal subduction (and/or spreading) rate has shown oscillations greater than 200 Myr
20 that are followed by sea level variation with a lag of ~30 Myr (van Andel, 1994). Secondly, it
21 must be mentioned that Shackleton (2000) has detected three different lags of 15, 7.6 and 3.7
22 Kyr of the ocean volume and climate responses to orbital forcing periodicities of 100, 41 and
23 21 Kyr (eccentricity, tilt or obliquity, and precession), respectively. While the geological lags
24 are due to mass inertia and volumetric readjustments of continents (van Andel, 1994), the
25 orbital scale lags are due mainly to the thermal and mass inertias associated with ice melting
26 of glaciers and polar ice-sheets (Shackleton, 2000). Although all of these lags are due to
27 different processes, they present a general common behavior in the TRM inertial responses
28 and must be included, at least empirically, in all climate models. These four pairs of
29 period/lag (P/L) samples of the climate lagged response processes are shown in Table C1.

1 Taking into account all of these aspects of C&SL variability, we propose that there is a lagged
2 millennial scale C&SL response, similar to the four described earlier, to the solar forcing
3 detected patterns of ~9500 yrs.

4

5 ***A proposed, applied and verified power law model for the climatic lags***

6 A power law model is proposed as follows:

7
$$L(t) = \alpha P^\beta, \quad (1)$$

8 Where, L is the period of the lagged response of the Earth's climate system, P is period of the
9 oscillatory forcing, α is the amplitude factor and β is the exponent of the power law.

10 Three power law models (Avg.-Std.Dev., Avg., and Avg+Std.Dev) are adjusted to Shackleton
11 (2000)'s evaluated lags of three different orbital forcing oscillations, and another lag
12 associated with plate tectonics (van Andel, 1994), and are displayed with the data of P/L pairs
13 in Figure C.1. Estimated parameters and equations are also displayed in this Figure.

14 Based on the obtained power law equations, we are able to estimate the lag corresponding to
15 the TSI ~9500 yr recurrent patterns. This lag must be located, following the power laws with
16 a probability of 63%, in the range from 1270 to 2120 yrs and with a central value of 1695 yrs.

17 Based also on the obtained power law equations, we have verified the cases of SL lag
18 analyses developed by Howard et al. (2015; hereafter H15) and van de Plassche et al. (2003;
19 hereafter vdP03). Firstly, in order to verify the forcing period of 12 yrs and the corresponding
20 lag of ~2 yrs estimated by H15, we look for the lag that corresponds to a forcing period of
21 12.6 yrs. The lag estimated with the power laws has a mean value of 2.5 and a range from 1.7
22 to 3.5 yrs, which includes the value estimated by H13.

23 Secondly, in order to estimate the forcing period corresponding to the lag of ~120 yrs
24 estimated by vdP03, we look for the forcing period of 650 yrs that corresponds to this lag
25 based on the estimated power law. We analyze the 10 Be record reconstructed by Bard et al.
26 (1997), which was employed by vdP03 in their simulated SL response to SA, based on
27 recurrent models. We apply two simple models, a sinusoidal model with a period of 650 yrs,
28 and an analog model with a lag of 647 yrs, which explain 17.6 and 32.7 % of the 10Be
29 variance, respectively, and are displayed in Figure C2, confirming the 650 yr provided by the
30 power law model.

1 It must be mentioned that the extrapolation of the Be10 record also provides a verification of
2 our solar forecast for the next centuries. See main text.

3

4 ***Iron deposition in the south-western Pacific [SWP] lags ~1500 yrs solar activity***

5 Based on the iron deposition in the SWP, off the Chilean coast, reconstructed record by Lamy
6 et al. (2001) and the SSN record by S04, a cross-correlation analysis was developed. Figure
7 C3a shows a maximum correlation of 0.6 (0.71) with the ~10 yr original resolution (smoothed
8 with 50yr-moving-average) records where the Fe signal lags 1570 yrs the SSN record. With
9 this lag, a linear lagged transformation was applied and a comparison of the Fe content record
10 and its model based on SSN are displayed in Figure C3b. The model explains more than 50%
11 of the variance in the Fe record.

12 In addition, we must also consider that there are natural oscillations in the THC, from years
13 and multi-decadal, to multi-centennial and multi-millennial scales, which appear in the multi-
14 millennia control runs of the OA-GCM (Jungclaus et al., 2010). In order to show this, we
15 have analyzed, with spectral analysis tools, data provided by the MPI climate-ocean group,
16 with main periodicity ranges of 4-7, 42-55, 180-260, 350-550, and 2600-3100 yrs (significant
17 level of 1%). See Figure C4.

18

19 ***Discussion***

20 With respect to a lagged climate, the historically detected existence of TRM inertias caused
21 by the ice-melting and thermo-haline circulation (THC) processes should be noted.

22 On the one hand, as Ahlman (1953) noted: “In a short preliminary review of the scientific
23 work of the Norwegian-British-Swedish expedition, E.F. Roots points out that the lag
24 between climatic change and change in form of the glaciers may be longer than the period of
25 climatic change itself.”

26 On the other hand, the THC, driven by meridional differences in temperature and salinity, is
27 considered as the main oceanic climate process (van Aken, 2007). It is initiated when the deep
28 waters, mainly forming in the North Atlantic, flow in the direction of the South Atlantic. At
29 about 60 degrees South, they join the Antarctic Circumpolar Current, in which they move
30 west to east, gradually rising towards the thermocline and spreading throughout the South

1 Atlantic, Pacific and Indian Oceans. The return of this massive flow to the North Atlantic
2 takes place through warm currents near the surface, whose circulation is linked to atmospheric
3 currents. The entire process can take from several hundred to thousands of years (van Aken,
4 2007).

5 The mean lag period, of 1695 +/- 425 years, associated with the ~9500 yr oscillation, is close
6 to double the period in which the CO₂ signal lags the hemispheric temperature signal during
7 the last glacial-interglacial cycle. For instance, Callion et al. (2003) have pointed out: “the
8 sequence of events during Termination III suggests that the CO₂ increase lagged Antarctic
9 deglacial warming by 800 +/- 200 years and preceded the Northern Hemisphere
10 deglaciation.... This result is in accordance with recent studies but, owing to our new method,
11 more precise.”

12

13 ***Conclusions***

14 We have proposed, applied and verified a simple power law model of the lagged response of
15 the ECS to different forcing phenomena during geological, orbital and suborbital time-scales.

16 The existence of these lagged responses is supported by simulated THC with one of the best
17 ECS long-term control runs (Jungclaus et al., 2010). These runs support the existence of
18 different, short and long-period, oceanic near-cyclic movements associated with the THC, and
19 implying, with moving sources and sinks of heat, mass and salt, several patterns of advection
20 of mass and heat that generate consequent patterns of: a) a thermal expansion/contraction of
21 sea-water, and then, a sea-level increase/decrease, and b) the transfer to/from the atmosphere
22 with a consequent increase/decrease of smelt of inland ice.

23 Based on the conclusion by Broecker and Henderson (1998) that “the Southern Ocean is
24 likely to be the main agent in the ~800 yr lag of atmospheric CO₂,” we propose, in addition to
25 the THC influences on the lagged climate responses, that the Southern Ocean should also be
26 considered as a main agent in these detected and suggested lags during the last millennia.

27 In order to corroborate these proposed lags, we are going to analyze C&SL records over the
28 Holocene looking for those associated with one of the most representative records of global
29 climate, the SL (see Appendix D).

30

1 **References**

2 van Andel, T.H. 1994. *New Views on an Old Planet*, 2nd Edition, Cambridge University
3 Press. ISBN 0521447550.

4 Ahlman, H.W.: *Glacier Variations and Climatic Fluctuations*, Bowman Memorial Lectures,
5 American Geographical Society, 51 pp, 1953.

6 van Aken, H.M. 2007. *The Oceanic Thermohaline Circulation—An Introduction*, Springer-
7 Verlag, Germany. Hardcover, xvii + 176 pages, 153 illustrations. ISBN 978-0-387-36637-1.

8 Bard, E., G. Raisbeck, F. Yiou, and J. Jouzel. 1997, Solar modulation of cosmogenic nuclide
9 production over the last millennium: comparison between ¹⁴C and ¹⁰Be records. *Earth and*
10 *Planetary Science Letters*, Vol. 150, pp. 453-462.

11 Broecker, W. S., and G. M. Henderson, The sequence of events surrounding Termination II
12 and their implications for the cause of glacial- interglacial CO₂ changes, *Paleoceanography*,
13 13, 352-364, 1998.

14 Caillon, N., Severinghaus, J.P., Jouzel, J., Barnola, J.-M., Kang, J. and Lipenkov, V.Y. 2003.
15 Timing of atmospheric CO₂ and Antarctic temperature changes across Termination III.
16 *Science* 299: 1728-1731.

17 Howard, D, Shaviv, NJ & Svensmark, H. 2015, The Solar and Southern Oscillation
18 Components in the Satellite Altimetry Data. *Journal of Geophysical Research: Space Physics*,
19 Vol. 120, pp. 3297-3306., 10.1002/2014JA020732.

20 van de Plassche, O., G. van der Schrier, S. L. Weber, W. R. Gehrels, and A. J. Wright. 2003.
21 Sea-level variability in the northwest Atlantic during the past 1500 years: A delayed response
22 to solar forcing?, *Gephys. Res. Lett.*, 30 (18), 1921, doi:10.1029/2003GL017558.

23 Shackleton, N.J. 1988: Oxygen isotopes, ice volume and sea level, *Quaternary Science*
24 *Reviews*, 6:183-190.

25

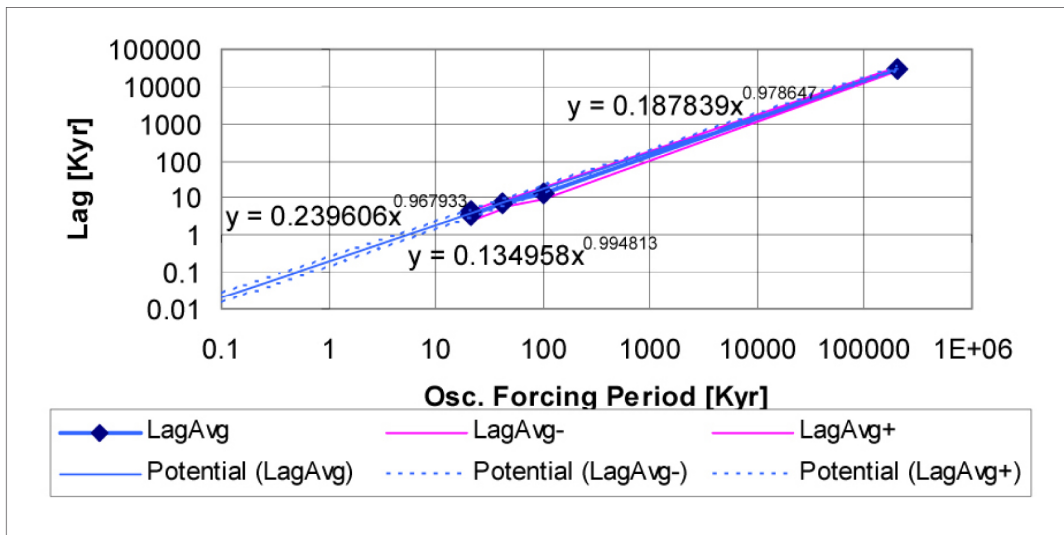
1 Table C1. Lags of different variables with respect to their different astronomical and tectonic
 2 forcing periods

Variable	Osc.ForcingPeriod [Kyr]	Lag(Avg) [Kyr]	Lag(Avg-s) [Kyr]	Lag(Avg+s) [Kyr]
d18OAir	21*	4.6*	4.2*	5*
d18OAir	41*	7*	5*	9*
IceVol.	100*	14*	9*	19*
Sea Level	100,000**	30,000**	27,000***	33,000***

3 *Shackleton (2000) and astronomical forcing, **van Andel (1994) and tectonic forcing,

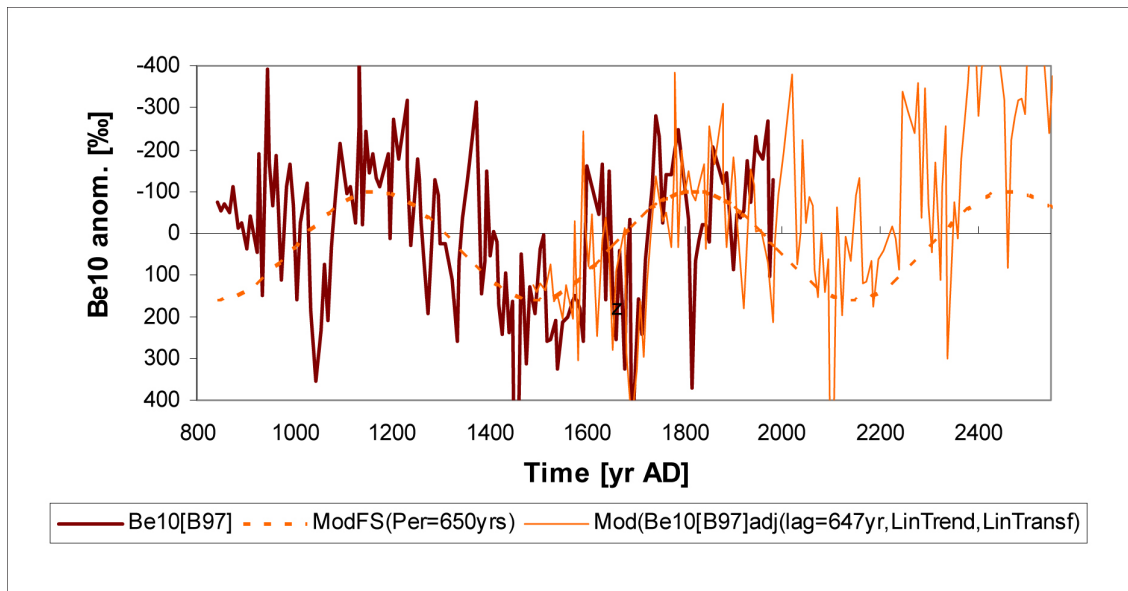
4 ***supposing a std.dev = 0.1avg.

5



1

2 Figure C1. Multiscale empirical model of climatic lagged response. Three power law models of lags, for the
 3 average and +/- standard deviation values, are displayed. Empirical models of lags in terms of climate oscillatory
 4 periods are adjusted to four estimations made by Shackleton (2000) and van Andel (1994). See data in Table C1.

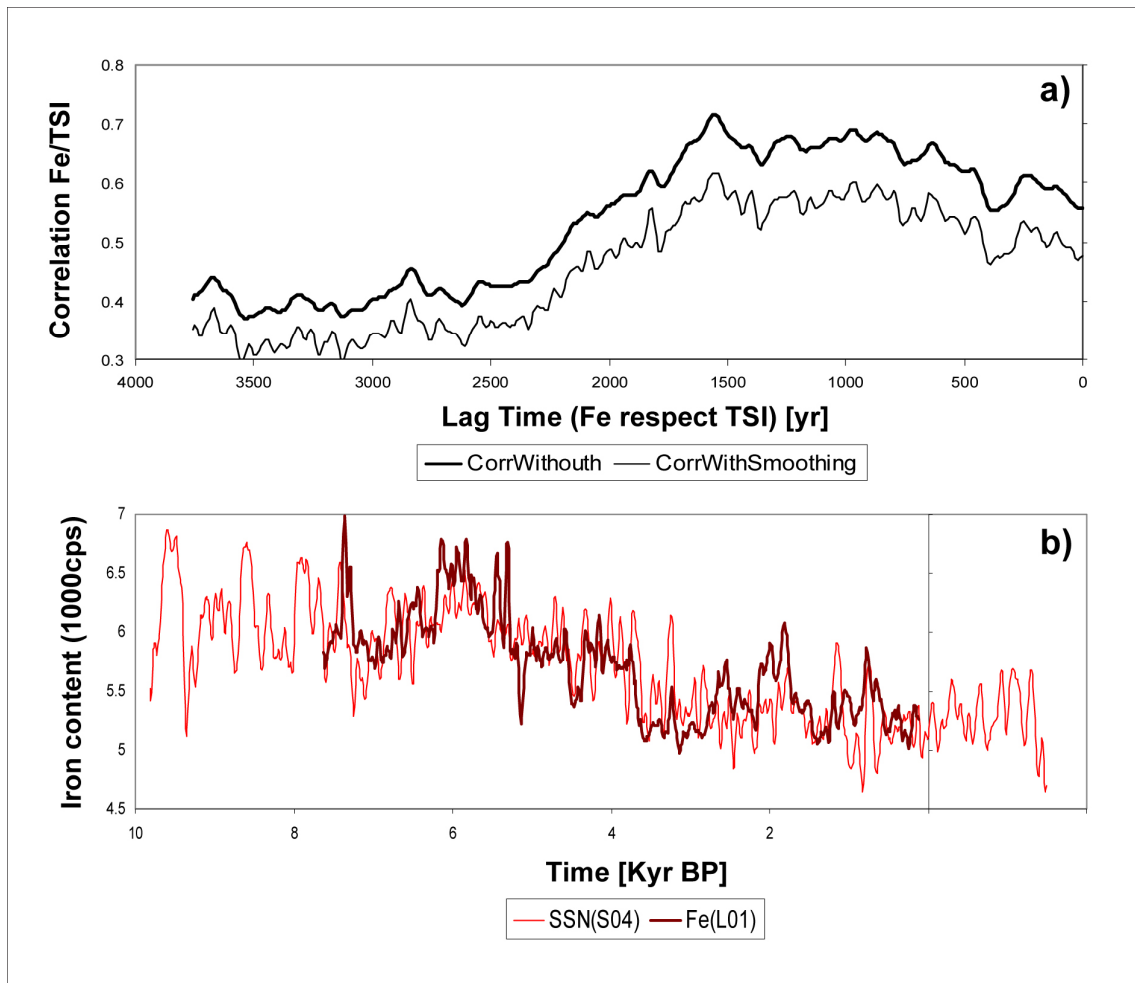


1

2

3 Figure C2. Double recurrent modelling of the Be10 record (Bard et al., 1997). A first model is based on a simple
 4 sine function with a period of 650 yrs, which explains 17% of the variance in the 10Be record. A second model is
 5 a simple analogue, which employs a lagged linear and trend adjustment with a lag of 647 yrs, explaining 33% of
 6 the variance in the 10Be record for the last four centuries. The vertical scale is inverted in order to indicate
 7 minimum and maxima of solar activity in the upper and lower parts of the graph, respectively.

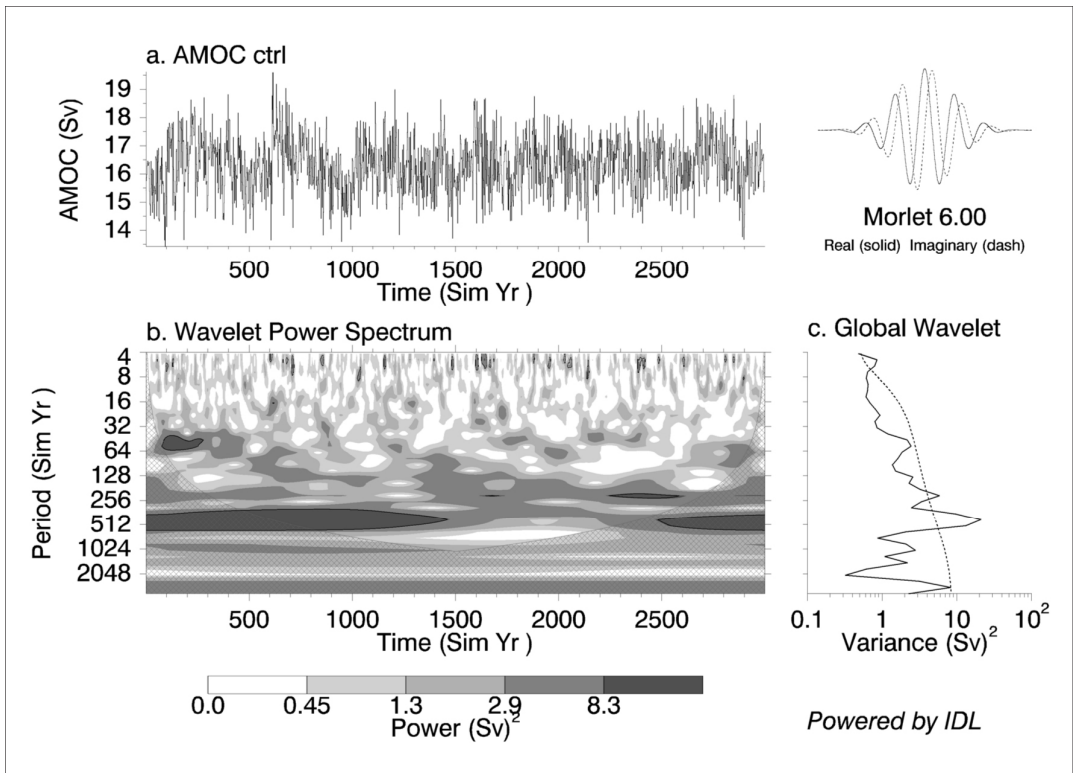
8



1

2

3 Figure C3. Lags and comparison between the south-western Pacific (SWP) iron deposition reconstructed by
 4 Lamy et al. (2001) and a proposed model based on the lagged influences of the SA SSN (S04). a) Lagged
 5 correlation values between SWP Fe deposition and TSI for different lags and two different resolutions of around
 6 10 and 50 yrs that show a maximum at a lag of 1570 yr, and b) The model is a simple analogue, which employs a
 7 lagged linear and trend adjustment with a lag of 1570 yrs, explaining 50% of the variance in the SWP Fe content
 8 record for the 8 last millennia.



1
2
3
4
5
6
7
8
9
10

Figure C4. (a) AMOC ctrl. (b) The wavelet power spectrum. The contour levels are chosen so that 75%, 50%, 25%, and 5% of the wavelet power is above each level, respectively. The cross-hatched region is the cone of influence, where zero padding has reduced the variance. Black contour is the 1% significance level, using a red-noise (autoregressive lag1) background spectrum. (c) The global wavelet power spectrum (black line). The dashed line is the significance for the global wavelet spectrum, assuming the same significance level and background spectrum as in (b). Reference: Torrence, C. and G. P. Compo, 1998: A Practical Guide to Wavelet Analysis. Bull. Amer. Meteor. Soc., 79, 61-78.

1 Appendix D: Sea level lags (~1600 yr) tropical climate

2

3 Sea level (SL) changes occur over a broad range of temporal scales and SL is strongly
4 correlated not only with climate but also with the diversity of life (van Andel, 1994). SL has
5 changed over geologic time up to hundreds of meters. As Hallam's (1984) Phanerozoic SL
6 reconstruction has shown, SL has changed with a maximum relative SL of +400 meters above
7 the present SL.

8 Although SL change has been considered as a result of many contributing processes, it can be
9 considered as an integral measure of climate change (Milne et al., 2009), with all its
10 complexity included. For instance, the primary contributors to contemporary sea level change
11 are the expansion of the ocean as it warms and the transfer of water currently stored on land to
12 the ocean, particularly from land ice (glaciers and ice sheets) (Church et al., 2013). Numerical
13 experiments with an ocean-atmosphere coupled model have shown that centennial variations
14 in the SL in the NW Atlantic may be associated with solar-forced variations of deep-ocean
15 salinities and temperature in the North Atlantic meridional overturning circulations (AMOC)
16 (van de Plassche et al., 2003; hereafter vdP03).

17 However, all of these complex aspects of SL variations and their lagged responses (see
18 Appendix C), can be better understood, if we analyze the phenomenon of SL changes as a
19 multi-scale, multi-process based on long-term scale information (Lovejoy and Schertzer,
20 2013).

21 In order to take into account the SL multi-fractal processes, firstly, we must consider that SL
22 change does not occur instantaneously after its different forcings. SL change takes time. This
23 has recently been emphasized by an important lag of ~120 yrs found between solar forcing
24 and its simulated SL variations (vdP03).

25 In order to promote a multi-fractal and lagged analysis of climate responses, and based on
26 non-linear relationships between pairs of periods of forcing oscillations and their SL lagged
27 responses, the author was able to estimate the climate & SL (C&SL) lag to the TSI forcing of
28 the 9500 +/- 100 yr recurrent patterns in Appendix C. This lag, which was estimated in line
29 with adjusted power laws, in a range from 1270 to 2120 yrs, is considered to be one of the
30 lagged processes associated with different, from geological and orbital to multi-millennial,
31 scales oscillations.

1 Another verification of the L/P power law profiles with SL information in the centennial scale
2 was developed in Appendix C. It was based on an analysis of a SL lag of 120 yrs published by
3 vdP03.

4 In the following paragraphs, we are going to: a) present SL reconstructed records and their
5 verification and adjustment, b) propose and apply a model for SL variations in term of the
6 lagged influences of CTC variations and their verification with their recurrences, c) discuss
7 results, and e) present the main conclusions.

8

9 ***The Holocene sea level record***

10 Primarily, we have chosen the Sidall et al. (2003; hereafter S03) SL reconstruction for the
11 Holocene and previous periods, because it is based on isotopic information coming from Red
12 Sea sediments and a multi-layer hydraulic model that considers evaporation due to high
13 surface temperatures. Complementarily, we selected the classic *Fairbridge curve* (FC), which
14 is a record of changes in sea levels over the past 10,000 years (Fairbridge, 1961; hereafter
15 F61). The FC, which is based on geological information of reefs and shorelines and the
16 effects of climate change upon them, shows periodic dips and spikes in levels against a larger
17 trend of rising ocean waters for the Holocene. Although the FC was developed more than 50
18 years ago, it was selected because its author also developed many excellent works and an
19 encyclopedic knowledge of not only geology and sea levels, but also paleo-climates, paleo-
20 environments, sedimentary geology, and solar system dynamics (Rampino, et al., 1987; Finkl,
21 1995). Both records are displayed in Fig. C1. Before their detailed comparison, we calculate
22 trends of both SL(F61) and SL(S03) records, and Figure D1 displays these trends.

23 A comparison of the detrended S(F61) and S(S03) records was developed. The S(S03) record
24 was compared with the adjusted S(F61). Two adjustments were applied to the S(F61), to force
25 the match between those records:

26 1) A temporal reduction factor of 0.97 was applied in order to minimize the RMS errors.
27 This adjustment is justified due to the well known ¹⁴C dating limitations in the 1950s
28 of the data employed in the S(F61) reconstruction.

29 2) A constant bias correction of the detrended value of S(F61) for the period 6-1.8 Kyr
30 BP.

31 The final verification/comparison process is displayed in Figure D2.

1 As we have mentioned in the main part, we have selected the Congo River basin surface air
2 temperature (CRB-SAT) signal, or T, as one of the records of regional climate most
3 influenced by the forcing of the sun. This T record is a continental tropical climate (CTC) that
4 is also influenced by volcanic activity. Additionally, it must be emphasized that volcanic
5 influences could be developed not only through blockage of atmospheric radiation effects, but
6 also through the deposition of ashes in CRB soils (Weijers, 2011).

7

8 *Simple models for lagged climate connections*

9 To take into account the lagged response of sea level to tropical climate variations, we
10 propose the following expression:

$$11 \quad S(t) = \alpha T(t - \delta) + \beta(t - t_1) + \gamma + e(t), \quad (D.1)$$

12 where, S is the sea-level values, T is the MAT-CRB values, α is a linear modulation factor
13 (>0 due to the positive, in general, correlation between T and SL changes), δ is a time lag
14 (>0), β is the temporal slope, γ is the additive constant, t_1 is the initial times for the modeled
15 periods, and $e(t)$ is the error.

16 To take into account the recurrent process of sea levels, we propose the following expression:

$$17 \quad S(t) = \alpha_S S(t - \delta) + \beta_S(t - t_1) + \gamma_S + e_S(t), \quad (D.2)$$

18 where, S is the sea-level values, α_S is a linear modulation factor (>0 due to the positive, in
19 general, correlation between T and SL changes), δ_S is a time lag (>0), β_S is the temporal
20 slope, γ_S is the additive constant, t_1 is the initial times for the modeled periods, and $e_S(t)$ is
21 the corresponding error.

22 We applied eq. D.1 to adjust a lagged CTC influence on the SL record. However, an
23 additional adjustment was applied to the S model to take into account potential negative
24 values of α during relatively short periods, when the T increase appears to cause not a
25 warming of sea water, but a possible ice and iceberg melting with a corresponding decrease of
26 deep-sea temperatures and a decrease in SL. These periods are supposedly short and located
27 in time, after a persisting cooling period. The corresponding graphics of these adjustments,
28 with and without melting effects, are displayed in Figure D3.

1 ***Verification and final adjustment of results***

2 In order to corroborate our model (and test our hypothesis), firstly, we verified the SL(T)
3 model.

4 To do that, we applied eq. D.2 to adjust a recurrence of the SL record. A lag of 9600 years
5 and linear adjustment were applied to the S analogue model to explain the last millennia and
6 to extrapolate it forward in time. Figure D4 presents a comparison of the model based on
7 tropical CTC information, with the analogue model S(S03) record, lagged 9600 years and
8 linearly adjusted.

9 This comparison constitutes a verification of the S modeling proposed as a lagged response of
10 CTC variability. The verification with the lagged SL record appears necessary because the
11 CTC response to the 1258 AD mega-volcanic-eruption seems to be influencing the initial low
12 temperatures but also, ~15 centuries later, a magnified decrease of sea level.

13 A final adjustment of our S model was applied for its recent values (reduction factor of 0.26)
14 based on another SL record of the last millennia from Iceland (Gehrels et al., 2006; hereafter
15 G06) based on different information and different techniques than S(S03). The comparison is
16 shown in Figure D5. Our non-adjusted or adjusted results suggest that the present increase in
17 SL is going to end in the next decades, and will be followed by a decreasing trend in sea
18 levels toward a value of 4 or 1 [m] below the present SL by 4000 AD, with oscillations of
19 around +/-1.6 or 0.4 [m], respectively.

20

21 ***Discussion***

22 In this section we will discuss different aspects of the lagged response of SL to the CTC:
23 firstly, the SL records; secondly, the lag of ~1500 yrs; and thirdly, the ~9500 yr recurrence of
24 the SL record.

25 With respect to a lagged climate, the historically detected existence of thermal, rheological
26 and mechanical inertias caused by ice-melting and thermo-haline circulation (THC) processes
27 should be noted, and have been discussed in Appendix C. In addition, the detected SL multi-
28 centennial lagged response can be justified and analyzed as a part of lagged response
29 processes and different climate oscillations detected previously.

1 On the one hand, Charles et al. (1996) found that Northern Hemisphere climate fluctuations
2 during the past 80 Kyr lagged those of the Southern Hemisphere by 1500 yr. Based on an
3 analysis of core RC11-83 in the Southern Atlantic (41°36'S; 9°48'E; 4718m), these authors
4 detected the early response of Southern Ocean surface and deep waters relative to
5 paleoceanographic proxies from other regions, a persistent pattern during the entire late
6 glacial-interglacial cycle. Additionally, in Appendix C we have detected a significant lagged
7 response of iron deposition in the SWP, off the Chilean coast, to the SSN solar signal, 1570
8 yrs later. These 1570-yr lags, almost coincide with the doubling of the lag shown by the CO₂
9 atmospheric concentration during the reconstructed last glacial-interglacial cycles.

10 On the other hand, there are climatic oscillations of around 1500 years. For instance, the
11 existence of climatic changes, possibly on a quasi-1,500-year cycle, is well established for the
12 last glacial period from ice cores. Bond et al. (1997) argue for a cyclicity close to 1470 ± 500
13 years in the North Atlantic region, and state that their results imply a variation in Holocene
14 climate in this region.

15 The analogue model of SL not only confirms the decreasing SL trend for the next millennia
16 based on the lagged influences of CTC and limits extreme decreases in SL, but also confirms
17 the possibly associated forcing oscillation of ~9500 yrs.

18 Additionally, in Appendix C we have also shown that there are natural oscillations in the
19 THC, from years and multi-decadal, to multi-centennial and multi-millennial scales, that
20 appear in the multi-millennia control runs of the OA-GCM (Jungclaus et al., 2010). Parts of
21 these cyclic circulations should be related to the detected lags of 2, 120 and 1500 yrs of the
22 SL response to solar forcing periods of 12.6, 650 and 9500 yrs, respectively. This is
23 confirmed because these lags are around half of the main periodic modes of natural oscillation
24 in the THC, with three of the period ranges of 4-7, 180-260, and 2600-3100 yrs, shown in
25 Figure C3.

26

27 ***Conclusions***

28 We have proposed a simple, power law model presented in Appendix C, for the lags of the
29 ECS that depend non-linearly on the forcing period. This model has been verified three times
30 with sea level response lags of 2, 120 and 1500 years, to the forcing periods of solar activity
31 of 12.6, 650 and 9500 yrs.

1 The natural THC variability shows periodic circulation cycles, and then favorable conditions
2 for generating stochastic resonances from other forcings. However, the temporal scale
3 similarities between THC cycles and the ECS lagged responses, also provide elements of
4 probable harmonic cycles of THC that could be linked to the lagged processes.

5 Specifically, based on the Broecker and Henderson (1998) conclusion that “the Southern
6 Ocean is likely to be the main agent in the ~800 yr lag of atmospheric CO₂,” and also on the
7 Charles et al. (1996) conclusion that “perhaps a more likely explanation for the observed
8 phase relationship involves tropical temperature variability,” we propose that the Southern
9 Ocean could also be the main agent, and the tropical ocean, the main source region, of this
10 millennia-scale SL lag during the Holocene.

11 Finally, we must emphasize that our SL model based on the lagged influence of tropical
12 climate is confirmed with the SL recurrent process with a lag of 9500 yrs, which also
13 confirms the proposed recurrent solar cycle of 9500 yrs and its influences in, at least, the
14 tropical climate and the global expressions of the ECS, the SL.

15

16 *References*

17 Ahlman, H.W. Glacier Variations and Climatic Fluctuations, Bowman Memorial Lectures,
18 American Geographical Society, 51 pp, 1953.

19 Broecker, W.S., and Henderson, G.M. The sequence of events surrounding Termination II
20 and their implications for the cause of glacial-interglacial CO₂ changes, *Paleoceanography*,
21 13, 352-364, 1998.

22 Caillon, N., Severinghaus, J.P., Jouzel, J., Barnola, J.-M., Kang, J. and Lipenkov, V.Y. 2003.
23 Timing of atmospheric CO₂ and Antarctic temperature changes across Termination III.
24 *Science* 299: 1728-1731.

25 Charles, C.D., LynchStieglitz, J., Ninnemann, U.S., and Fairbanks, R.G. 1996. Climate
26 connections between the hemispheres revealed by deep sea sediment core ice core
27 correlations. *Earth and Planetary Science Letters*. 142:19-27. 10.1016/0012-821x(96)00083-
28 0.

29 Church, J.A., Clark, P.U., Cazenave, A., Gregory, J.M., Jevrejeva, S., Levermann, A.,
30 Merrifield, M.A., Milne, G.A., Nerem, R.S., Nunn, P.D., Payne, A.J., Pfeffer, W.T., Stammer,

1 D., and Unnikrishnan, A.S. 2013. Sea Level Change. In: Climate Change 2013: The Physical
2 Science Basis. Contribution of Working Group I to the Fifth Assessment Report of the
3 Intergovernmental Panel on Climate Change [Stocker, T.F., Qin, D., Plattner, G.K., Tignor,
4 M., Allen, S.K., Boschung, J., Nauels, A., Xia, Y., Bex, V., and Midgley, P.M. (eds.)].
5 Cambridge University Press, Cambridge, United Kingdom and New York, NY, USA.

6 Fairbridge, R.W. 1961. Eustatic changes in sea level, *Phys.Chem. Earth*, 5:99.

7 Fairbridge, R.W. and Sanders, J.E. 1987. The Sun's Orbit, A.D. 750-2050: basis for new
8 perspectives on planetary dynamics and Earth-Moon linkage. In: Rampino, M.R., Sanders,
9 J.E., Newman, W.S., and Konigsson, L.K. 1987. *Climate: History, Periodicity, and*
10 *Predictability*. Van Nostrand Reinhold USA, pp. 446 to 471.

11 Finkl, C.W., (Ed.). 1995. *Holocene cycles: Climate, sea levels, and sedimentation*.
12 *Charlottesville, Va: Coastal Education and Research Foundation. (A special issue of the*
13 *Journal of Coastal Research—Being a Jubilee Volume in Celebration of the 80th Birthday of*
14 *Rhodes W. Fairbridge).*

15 Gehrels, W.R. et al. 2006. Rapid sea-level rise in the North Atlantic Ocean since the first
16 half of the nineteenth century. *Holocene* 16:949–965.

17 Hallam, A. 1984. Pre-Quaternary Sea-Level Changes. *Ann. Rev. Earth Planet. Sci.* 12: 205-
18 243.

19 Kemp, A.C., Horton, B.P., Donnelly, J.D., Mann, M.E., Vermeer, M. and Rahmstorf, S. 2011.
20 Climate related sea-level variations over the past two millennia. *Proceedings of the National*
21 *Academy of Sciences* 108, Pg 11017-11022.

22 Lovejoy, S. and Schertzer, D. 2013. *The Weather and Climate: Emergent Laws and*
23 *Multifractal Cascades*, Cambridge U. Press, 496 pp.
24 <http://www.physics.mcgill.ca/~gang/ftp.transfer/final.book.figs.Feb.2012.pdf>

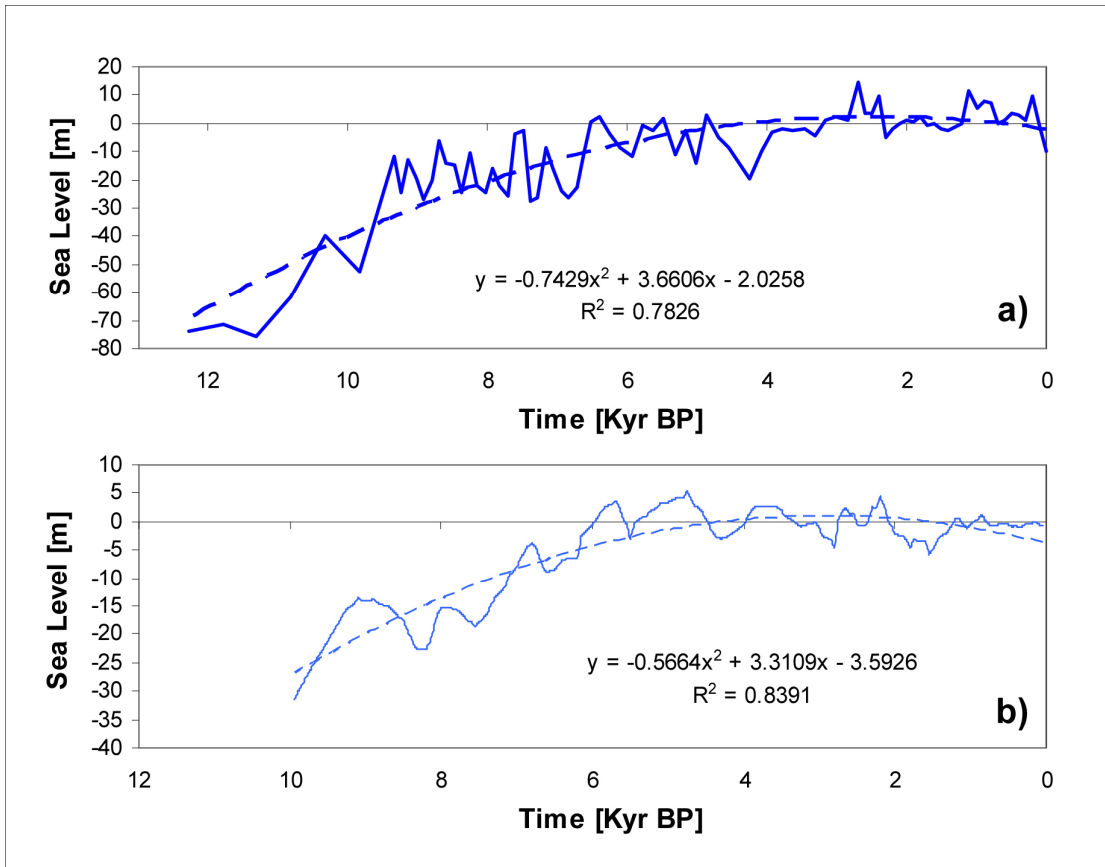
25 Munk, W. 2002. Twentieth century sea level: An enigma, *Proc. Nat. Acad. Sci.*, 99, 6550–
26 6555.

27 Milne, G.A., Gehrels, W.R., Hughes, C.W., and Tamisiea, M.E. 2009. Identifying the causes
28 of sea-level change. *Nature Geosci*, 2, 471–478.

29 Mörner, N-A, 1995. Sea Level and Climate—The decadal-to-century signals. *J Coastal Res.*,
30 *Special Issue No.17: Holocene cycles, Sea Levels and Sedimentation*, pp. 261-268.

- 1 Rahmstorf, S. 2007. A Semi-Empirical Approach to Projecting Future Sea-Level Rise.
2 Science, 315, 368-370.
- 3 Rampino, M.R., Sanders, I.E., Newman, W.S. and Konigsson, L.K. (Eds.). 1987. Climate:
4 History, Periodicity, and Predictability, Van Nostrand Reinhold, New York. (Papers presented
5 at a meeting held May 21-23, 1984, at Barnard College, Columbia University, to honor
6 Professor Emeritus Rhodes W. Fairbridge on his 70th birthday).
- 7 Sánchez-Sesma, J. 2010. Technical Note: Multi-centennial scale analysis and synthesis of an
8 ensemble mean response of ENSO to solar and volcanic forcings, *Clim. Past Discuss.*, 6,
9 2055-2069, 2010.
- 10 Shackleton, N.J. 1988. Oxygen isotopes, ice volume and sea level, *Quaternary Science*
11 *Reviews*, 6:183-190.
- 12 Siddall, M., Rohling, E.J., Almogi-Labin, A., Hemleben, Ch., Meischner, D., Schmelzter, I.,
13 and Smeed, D.A. 2003. Sea-level fluctuations during the last glacial cycle. *Nature* 423: 853-
14 858.
- 15 Siddall, M., Rohling, E.J., Almo gl-Lab. In: A., Hemleben, Ch., Melschner, D., Schmelzer, I.,
16 and Smeed, D.A. 2003. Sea-level fluctuations during the last glacial cycle. *Nature* 243, 853-
17 858.
- 18 Stacey, C. 1963. Cyclical measures: Some tidal aspects concerning equinoctial years.
19 *Annals New York Academy of Science* 105, Article 2:421-460.
- 20 Ters, M. 1987. Variations in Holocene sea level on the French Atlantic coast and their
21 climatic significance. In: Rampino, M.R., Sanders, J.E., Newman, W.S. and Konigsson, L.K.
22 (Eds.). *Climate: History, Periodicity, and Predictability*. Van Nostrand Reinhold, New York,
23 NY, pp. 204-236.
- 24 van Andel T.H. 1994. *New Views on an Old Planet*, 2nd Edition, Cambridge University
25 Press. ISBN 0521447550.
- 26 van Aken, H.M. 2007. *The Oceanic Thermohaline Circulation—An Introduction*, Springer-
27 Verlag, Germany. Hardcover, xvii + 176 pages, 153 illustrations. ISBN 978-0-387-36637-1.
- 28 Weijers, J.W.H., Schefuss, E., Schouten, S., and Damste, J.S.S. 2007. Coupled thermal and
29 hydrological evolution of tropical Africa over the last deglaciation. *Science*, 315, 1701-1704.

- 1 Vermeer, M. and Rahmstorf, S. 2009. Global sea level linked to global temperature. Proc Natl
- 2 Acad Sci USA 106:21527–21532.

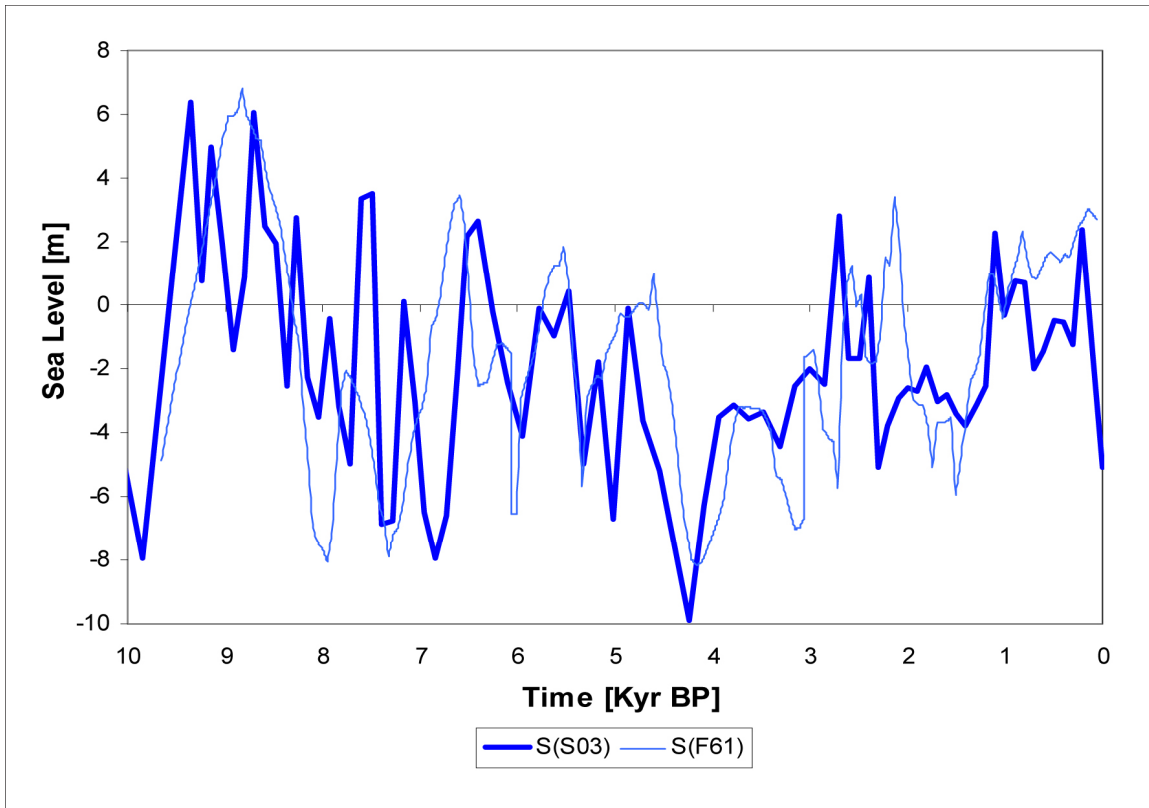


1

2

3 Figure D1. Millenia-scale reconstructed records of relative sea-level, S , by a) Sidall et al. (2003), $S(S03)$, and

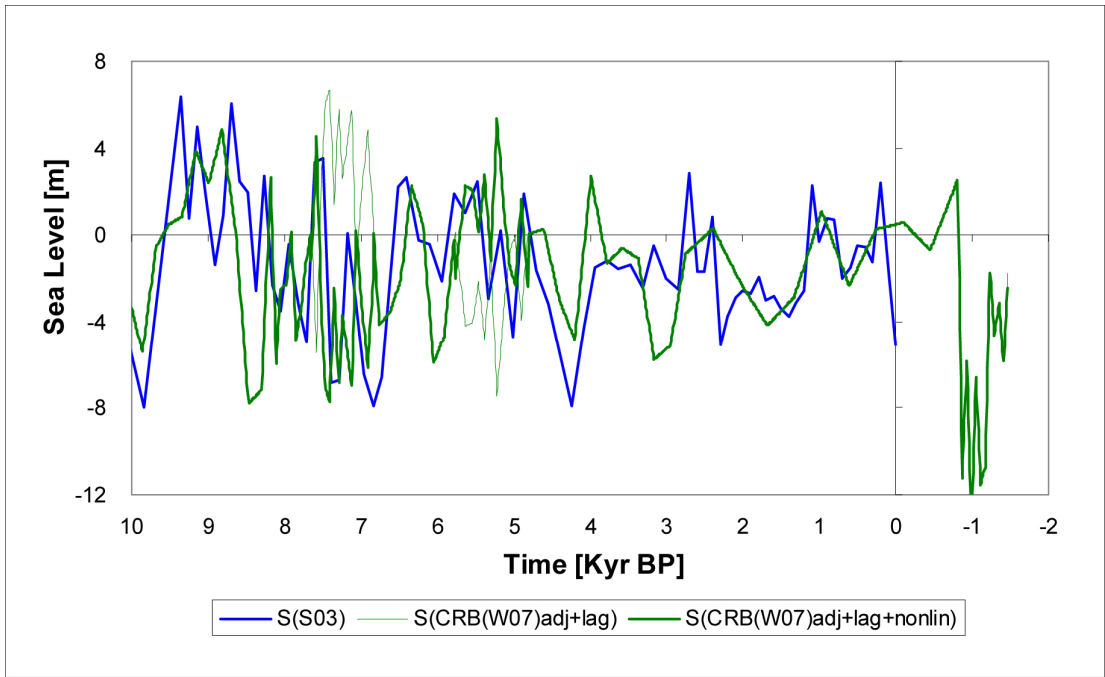
4 b) Fairbridge (1961), $S(F61)$. Polynomials trends are also displayed.



1

2

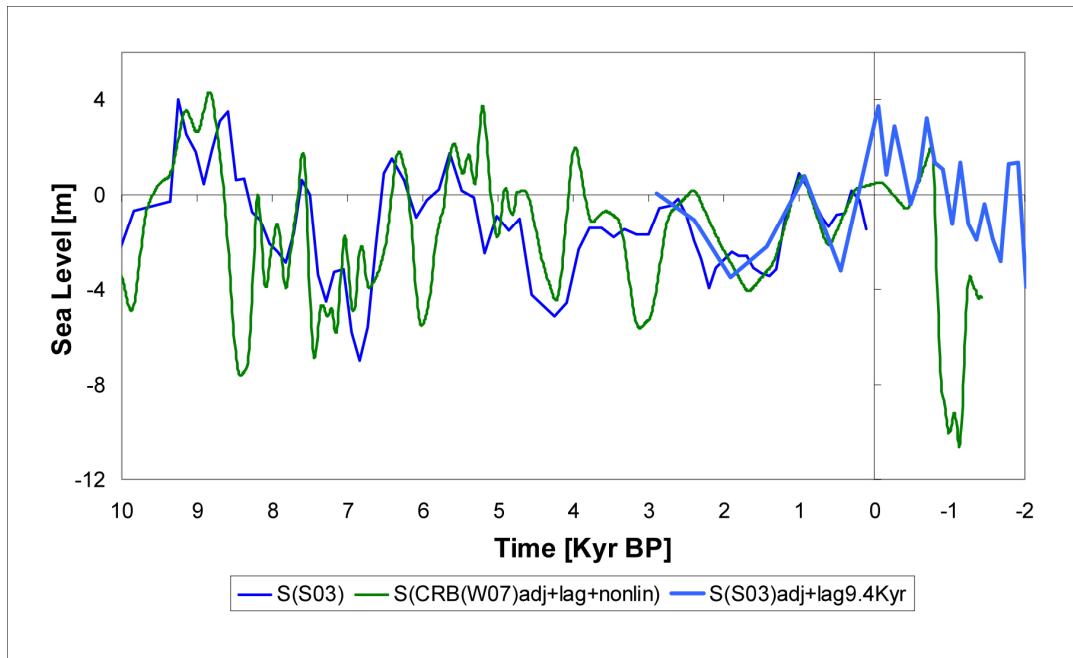
3 Figure D2. Comparison of two sea-level records: the S(S03) and the adjusted S(F61). Two adjustments were
4 applied to the S(F61) reconstruction: a time reduction factor (0.89) and a simple constant bias adjustment
5 between 5 and 3.8 Kyr BP. The adjusted S(F61) reconstruction shows a very good match with the S(S03) record.



1

2

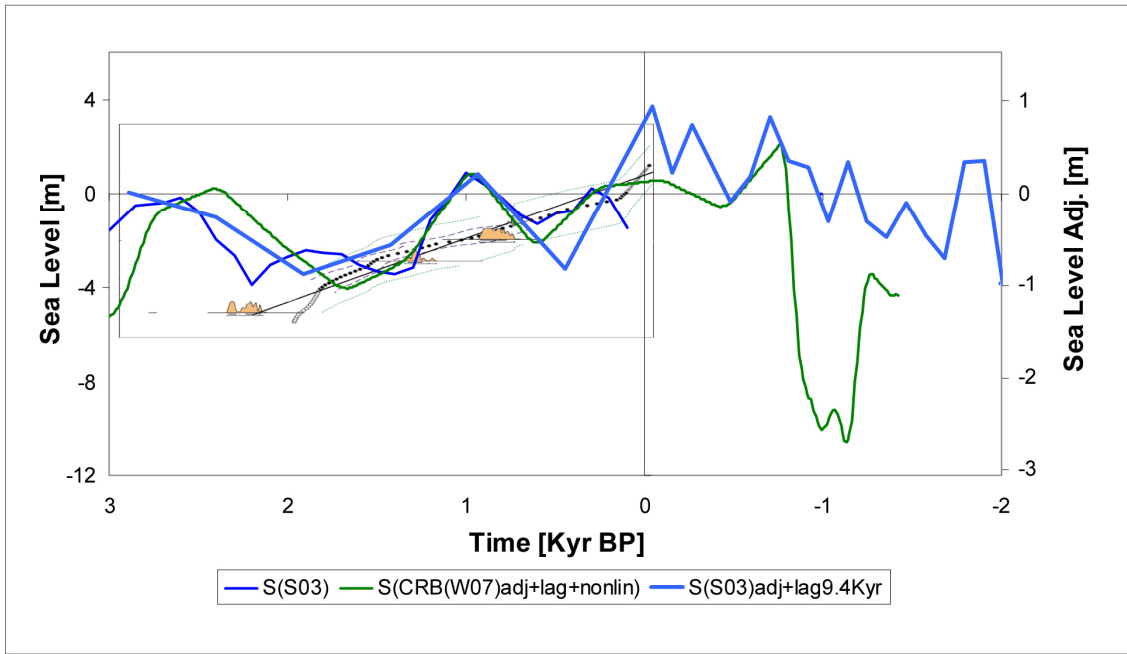
3 Figure D3. Comparison reconstructed and modelled sea-level records. The reconstructed record is developed by
 4 S03, and is compared with the lagged linear analogue transformation of the CRB SAT record. The CRB SAT
 5 record is shown a) without and b) with an adjustment of change of sign in the temporal ranges from 7.4 to 6.8
 6 and 5.8 to 5 Kyr BP.



1

2

3 Figure D4. Comparison of reconstructed and modelled sea-level records. The reconstructed record is developed
 4 by S03, and is compared with the smoothed linear analogue transformation of the CRB SAT record and with a
 5 lag of ~1500 yrs and partially non-linearly adjusted (see Fig. D3), and an analogue (linear transformation and
 6 trend adjustment) model based on the same S03 record with a lag of 9.6 Kyr.



1

2

3 Figure D5. Comparison/calibration of results shown in Figure D4 with other SL reconstructions (Gehrald et al.,
 4 2007). The graphics shows two scales for the SL: one is the original S03 SL scale (left), and the other is the
 5 adjusted one (right) with a recent published reconstruction (dots and the linear trend depicted, and the right scale
 6 are taken from Gehrald et al., 2007).

7

1 Acknowledgements

2 This work was motivated by Rhodes Fairbridge's work around the idea that the solar system
3 regulates the solar and Earth's climate (Mackey, 2006). The author thanks Professor Jan
4 Veizer for his encouraging comments. The author also thanks Jana Schroeder, for her editorial
5 contributions, and Oscar Alonso and Ricardo Espinoza, for their graphical contributions to
6 this work. This work was initiated when the author was supported (2008-2012) by a NSF
7 grant (GEO-0452325) through the IAI project CRN-II-2050 and by the Institute UC MEXUS
8 and CONACYT through an international collaborative project between IMTA and SIO/UCSD
9 under the 2008 Climate Change Program.

10
11 References

12 Abreu J.A., C. Albert, J. Beer, A. Ferriz-Mas., K. G. McCracken, and F. Steinhilber (2012), Is
13 there a planetary influence on solar activity? *Astronomy and Astrophysics*, 548, A88.

14 A. Berger, M. F. Loutre, and J. L. Mélice (2006), Equatorial insolation: from precession
15 harmonics to eccentricity frequencies, *Clim. Past*, 2, 131–136, [www.clim-](http://www.clim-past.net/2/131/2006/)
16 [past.net/2/131/2006/](http://www.clim-past.net/2/131/2006/)

17 Charvátová, I. (1995), Solar-terrestrial and climatic variability during the last several
18 millennia in relation to solar inertial motion, *J. Coastal Res.*, 17, 343-354.

19 Charvátová, I. (2000), Can origin of the 2400-year cycle of solar activity be caused by solar
20 inertial motion? *Ann. Geophys.*, 18, 399-405.

21 Cuffey, K. M., and G. D. Clow (1997), Temperature, accumulation, and ice sheet elevation in
22 central Greenland through the last deglacial transition, *Journal of Geophysical Research*,
23 102:26383-26396.

24 Duhau, S. and C. de Jager (2010), The Forthcoming Grand Minimum of Solar Activity,
25 *Journal of Cosmology*, 8, 1983-1999.

26 Eddy, J. A. (1981), Climate and the Role of the Sun, in *Climate and History*, (R. I. Rotberg
27 and T. K. Rabb, Eds.) Princeton University Press, Princeton, New Jersey, 145-168.

28 Fairbridge, R. W., and J. E. Sanders (1987), The Sun's orbit AD 750-2050. Basis for new
29 perspectives on planetary dynamics and Earth-Moon linkage, in: Rampino, M. R., J. E.

1 Sanders, W. S. Newman, and L. K. Königsson, (eds.), *Climate, history and predictability*, Van
2 Nostrand-Reinhold, New York, 446-471.

3 Fairbridge, R. W., and J. H. Shirley (1987), Prolonged minima and the 179-yr cycle of the
4 solar inertial motion, *Sol. Phys.*, 110, 191-220.

5 Finkel, R. C., and K. Nishiizumi (1997), Beryllium 10 concentrations in the Greenland Ice
6 Sheet Project 2 ice core from 3-40 ka, *Journal of Geophysical Research*, 102:26699-26706.

7 Fowler, W. (1972), What Cooks with Solar Neutrinos? *Nature*, 238, 24-26;
8 doi:10.1038/238024a0.

9 Haigh J. D. (2011), *Solar Influences on Climate*, Grantham Institute for Climate Change
10 Briefing Paper No 5, Imperial College, London.

11 IPCC (2013), *Climate Change 2013: The Physical Science Basis. Contribution of Working*
12 *Group I to the Fifth Assessment Report of the Intergovernmental Panel on Climate Change*
13 [Stocker, T. F., D. Qin, G. K. Plattner, M. Tignor, S. K. Allen, J. Boschung, A. Nauels, Y.
14 Xia, V. Bex, and P. M. Midgley (eds.)]. Cambridge University Press, Cambridge, United
15 Kingdom and New York, NY, USA, 1535 pp.

16 Jose, P. D. (1965), Sun's Motion and Sunspots, *Astron. J.*, 10(1), 193-200.

17 Kindler, P., Guillevic, M., Baumgartner, M., Schwander, J., Landais, A., and Leuenberger,
18 M.: Temperature reconstruction from 10 to 120 kyr b2k from the NGRIP ice core, *Clim. Past*,
19 10, 887-902, doi:10.5194/cp-10-887-2014, 2014.

20 Landscheidt, T. (1999), Extrema in sunspot cycle linked to Sun's motion, *Sol. Phys.*, 189, 413-
21 424.

22 Laskar, J., A. Fienga, M. Gastineau, and H. Manche (2011), La2010: A new orbital solution
23 for the long-term motion of the Earth, *Astronomy & Astrophysics*, 532 (A889).

24 Mackey, R. (2007), Rhodes Fairbridge and the idea that the solar system regulates the Earth's
25 climate, *Journal of Coastal Research*, Special Issue 50 (Proceedings of the 9th International
26 Coastal Symposium), 955 - 968. Gold Coast, Australia.

27 Muscheler, R., and U. Heikkilä (2011), Constraints on long-term changes in solar activity
28 from the range of variability of cosmogenic radionuclide records, *Astrophys. Space Sci.*
29 *Trans.*, 7, 355-364, doi:10.5194/astra-7-355.

1 Perry, C. A., and K. J. Hsu (2000), Geophysical, archaeological, and historical evidence
2 support a solar-output model for climate change. *Proceedings of the National Academy of*
3 *Sciences USA*, 97, 12,433-12,438.

4 Peeters, F. J. C., R. Achinson, G. J. A. Brummer, W. P. M. de Ruijter, G. M. Ganssen, R. R.
5 Schneider, E. Ufkes, and D. Kroon (2004), Vigorous exchange between Indian and at the end
6 of the last five glacial periods, *Nature*, 430, 661-665.

7 Piotrowski, A. M., S. L. Goldstein, S. R. Hemming, and R. G. Fairbanks (2004),
8 Intensification and variability of ocean thermohaline circulation through the last deglaciation,
9 *Earth and Planetary Science Letters*, 225, 205-220.

10 Ruzmaikin, A. A. (1983), Nonlinear problems of the solar dynamo, in: Soward, A. M. (ed.):
11 *Stellar and Planetary Magnetism*, Gordon Breach, New York, 151.

12 Schmitt, D., M. Schussler, and A. Ferriz-Mas (1996), Intermittent solar activity by an on-off
13 dynamo, *Astron. Astrophys.*, 311, L1.

14 Sánchez-Sesma, J. (2015), The climates of history and their influences on the world
15 population: A hypothesis, test and millennia scale projections, *Proceedings of the National*
16 *Academy of Sciences* (sent).

17 Shaviv N. J., A. Prokoph, and J. Veizer (2014), Is the solar system's galactic motion imprinted
18 in the Phanerozoic climate?, *Sci Rep.*, Aug 21;4:6150. doi: 10.1038/srep06150.

19 Solanki, S. K., I. G. Usoskin, B. Kromer, M. Schüssler, and J. Beer (2004), Unusual activity
20 of the Sun during recent decades compared to the previous 11,000 years, *Nature*, Vol. 431,
21 No. 7012, 1084–1087.

22 Steinhilber, F., J. Beer, and C. Frohlich (2009), Total solar irradiance during the Holocene,
23 *Geophysical Research Letters*, 36, doi: 10.1029/2009GL040142.

24 Steinhilber, F., J. A. Abreu, J. Beer, I. Brunner, M. Christl, H. Fischer, U. Heikkilä, P. W.
25 Kubik, M. Mann, K. G. McCracken, H. Miller, H. Miyahara, H. Oerter, and F. Wilhelms
26 (2012), 9,400 years of cosmic radiation and solar activity from ice cores and tree rings, *Proc.*
27 *Natl. Acad. Sci. USA*, 109. 10.1073/pnas1118965109.

28 Steinhilber F., and J. Beer (2013), Prediction of solar activity for the next 500 years, *J.*
29 *Geophys. Res. Space Physics*, 118, doi:10.1002/jgra.50210.

- 1 Shirley, J. H., and R. W. Fairbridge (Eds.) (1997), *Encyclopedia of Planetary Sciences*,
2 Chapman & Hall.
- 3 Stacey, C. (1967), Earth motions and time and astronomic cycles. Pages 335-340 and 999-
4 1003 in *The Encyclopedia of Atmospheric Sciences and Astrogeology*, R. Fairbridge, editor,
5 Reinhold Publishing, NewYork.
- 6 Stacey, C. M. (1963), Cyclic measure. Some tidal measures concerning equinoctal years, *Ann.*
7 *New York Acad. Sciences*, No. 6.
- 8 Sturevik-Storm, A. et al. (2014), ^{10}Be climate fingerprints during the Eemian in the NEEM
9 ice core, Greenland, *Nature/Sci.Rep.*, 4, 6408; DOI:10.1038/srep06408.
- 10 Torrence, C., and G. P. Compo (1998), A Practical Guide to Wavelet Analysis, *B. Am.*
11 *Meteorol. Soc.*, 79, 61-78.
- 12 Velasco Herrera, V. M., B. Mendoza, and G. Velasco Herrera (2015), Reconstruction and
13 prediction of the total solar irradiance: From the Medieval Warm Period to the 21st century,
14 *New Astronomy*, 34, 221, DOI: 10.1016/j.newast.2014.07.009
- 15 Weijers, J. W. H., E. Schefuß, S. Schouten, J. S. Sinninghe Damsté (2007), Coupled thermal
16 and hydrological evolution of tropical Africa over the last deglaciation. *Science*, 315, 1701-
17 1704.
- 18 Xapsos, M., and E. Burke (2009), Evidence of 6000-year periodicity in reconstructed sunspot
19 numbers, *Sol. Phys.*, 257 (2), 363-369.
- 20 Clarke, A.; Church, J.; Gould, J. (2001). Ocean processes and climate phenomena, in: Siedler,
21 G. et al. (Ed.) (2001). *Ocean circulation and climate: observing and modelling the global*
22 *ocean. International Geophysics Series, 77: pp. 11-30*
- 23 Usoskin, I.G., Hulot, G., Gallet, Y., Roth, R., Licht, A., Joos, F., Kovaltsov, G.A., Thebault,
24 E. and Khokhlov, A. 2014. Evidence for distinct modes of solar activity. *Astronomy and*
25 *Astrophysics* 562: L10, doi: 10.1051/0004-6361/201423391.
- 26 Janardhan P., Bisoi, S.K., Gosain S. 2010. Solar Polar Fields During Cycles 21 \square - \square 23:
27 Correlation with Meridional Flows, *Solar Physics*, December 2010, Volume 267, Issue 2, pp
28 267-277, doi: 10.1007/s11207-010-9653-x.
- 29 Janardhan, P., Bisoi, S.K., Ananthakrishnan, S., Tokumar, M., and Fujiki, K. 2011. The
30 prelude to the deep minimum between solar cycles 23 and 24: Interplanetary scintillation

1 signatures in the inner heliosphere, *Geophys. Res. Lett.*, 38, L20108,
2 doi:10.1029/2011GL049227.

3 Janardhan, P., Bisoi S.B., Ananthakrishnan, S., Tokumaru, M., Fujiki, K., Jose, L., and
4 Sridharan, R. 2015. A 20 year decline in solar photospheric magnetic fields: Inner-
5 heliospheric signatures and possible implications, *J. Geophys. Res.: Space Physics*, 120(7),
6 5306–5317, doi: 10.1002/2015JA021123.

7 Janardhan, P., Bisoi S.B., Ananthakrishnan, S., Sridharan, R., and Jose, L. 2015. Solar and
8 Interplanetary Signatures of a Maunder-like Grand Solar Minimum around the Corner -
9 Implications to Near-Earth Space, Sun and Geosphere, Special Issue: UN/Japan Workshop on
10 SPACE WEATHER (In Press).

11 Choudhuri, A.R. and Karak, B.B. 2012. The origin of grand minima in the sunspot cycle,
12 *Phys.Rev. Lett.*, 109,171103.

13 Karak, B.B. and Choudhuri, A.R. 2011. Is meridional circulation important in modelling
14 irregularities of the solar cycle? Comparative Magnetic Minima: characterizing quiet times in
15 the Sun and stars. Proceedings IAU Symposium No. 286, 2011, A.C. Editor, B.D. Editor &
16 C.E. Editor, eds. International Astronomical Union.

17 Hathaway D.H. and Rightmire, L. 2010. Variations in the Sun's Meridional Flow over a Solar
18 Cycle, *Science*, Vol. 327, No. 5971, pp. 1350-1352, doi: 10.1126/science.1181990.

1 Figure Legends

2 Figure 1. Solar-related and climate signals. (a) Solar activity, TSI, reconstructed by S04, S09
3 and S12, after an intercalibration using the S09 record as a base. (b) ^{10}Be isotope
4 concentration in polar ice cores during the past 130 Kyr (Finkel and Nishiizumi, 1997;
5 Stuverik-Storm et al., 2014). (c) The continental tropical Congo River basin (CRB) mean
6 annual surface air temperature record for the last 21000 years, based on lipids (W07). Please
7 note that in all figures: as the ^{10}Be concentration varies inversely with Solar activity, TSI, the
8 beryllium scale is inverted, and thus upper parts in this scale indicate high TSI levels.

9 Figure 2. Data and modelling of ^{10}Be isotope concentration in Greenland ice cores. a) Data
10 and a FS model of ^{10}Be isotope for the past 40 Kyr provided by FN97 (Finkel and
11 Nishiizumi, 1997) after detrended and demodulated. b) The model, shown in a), is
12 extrapolated covering the last 135 Kyr, and the SS14 (Stuverik-Storm et al., 2014) data is
13 included for comparison. c) A zoom of b) for a detailed comparison of the extrapolated FS
14 model and the SS14 data. Please note that a maximum match implies a SS14 temporal
15 adjustment, or time bias, of 1.5 Kyr going back in time.

16 Figure 3. A test of the recurrent TSI signal based on ^{14}C over the last 11000 yrs, TSI(S04),
17 and the ^{10}Be isotope concentration record from Greenland ice cores. a) Extrapolated
18 TSI(S04) record backward in time, 9400 yrs, and its model based on ^{10}Be isotope (A14) that
19 covers the period from 18000 to 10000 yrs BP. b) The residue of model, smoothed with a
20 100-yr-moving-average process, shown in a), is also explained, with an analogue non-linear
21 model, with a lag of ~ 1550 yrs, and a change of sign that is only applied for the first 1500 yrs.

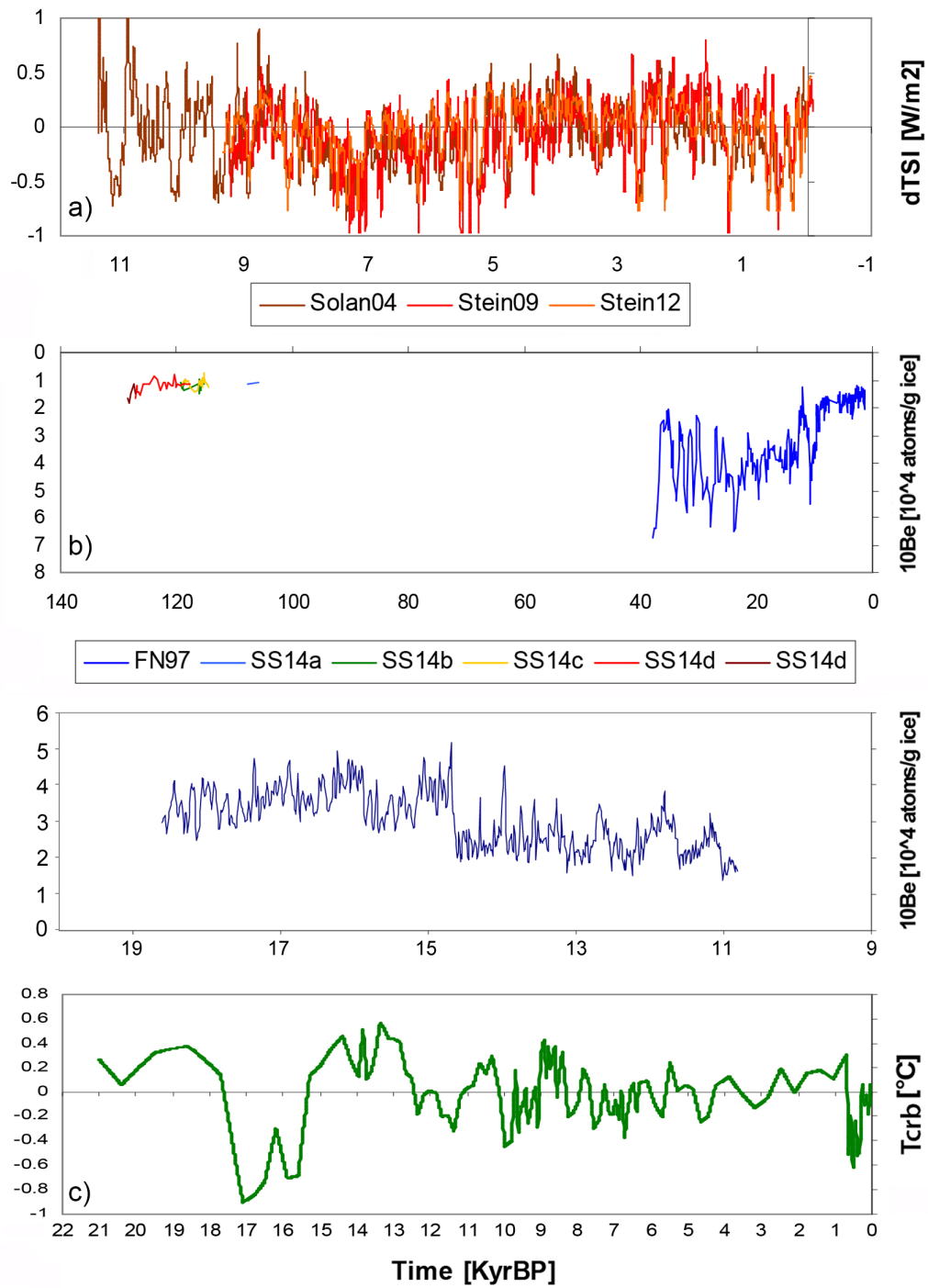
22 Figure 4. Solar activity signals reconstructed and modelled records. (a) Solar activity, TSI,
23 reconstructed by S04, S09 and S12, shown in Figure 1a, and their analogue models. (b) A
24 zoom of a) that covers only 2Kyr. (c) Another greater zoom of a) that covers only 0.85Kyr
25 including the independent TSI forecast by S13. (d) The CTC Tcrb signal and its simple model
26 including the independent TSI forecast by S13. Big and small vertical arrows indicate Super
27 and Grand solar minima.

28 Figure 5. Tropical climate (CRB) T reconstructed and detrended signal and its solar-based
29 models. The CRB T models, extrapolated backward in time, were based on: a) TSI (S04), b)
30 TSI (S09) and c) TSI (S12), applying Eq. 2 with greater modulated amplitudes before 10Kyr
31 BP.

1 Figure 6. Continental tropical climate, T_{crb} reconstructed and its analogue model with a lag
2 of 9.6 Kyrs but including two forecasts of TSI, provided by our analogue model TSI (S04)
3 and the TSI forecast by S13. (a) The CRB T signal and its model, during the last 1 and future
4 1 Kyr, and (b) a zoom of a) during the last 0.3 and future 0.6 Kyr.

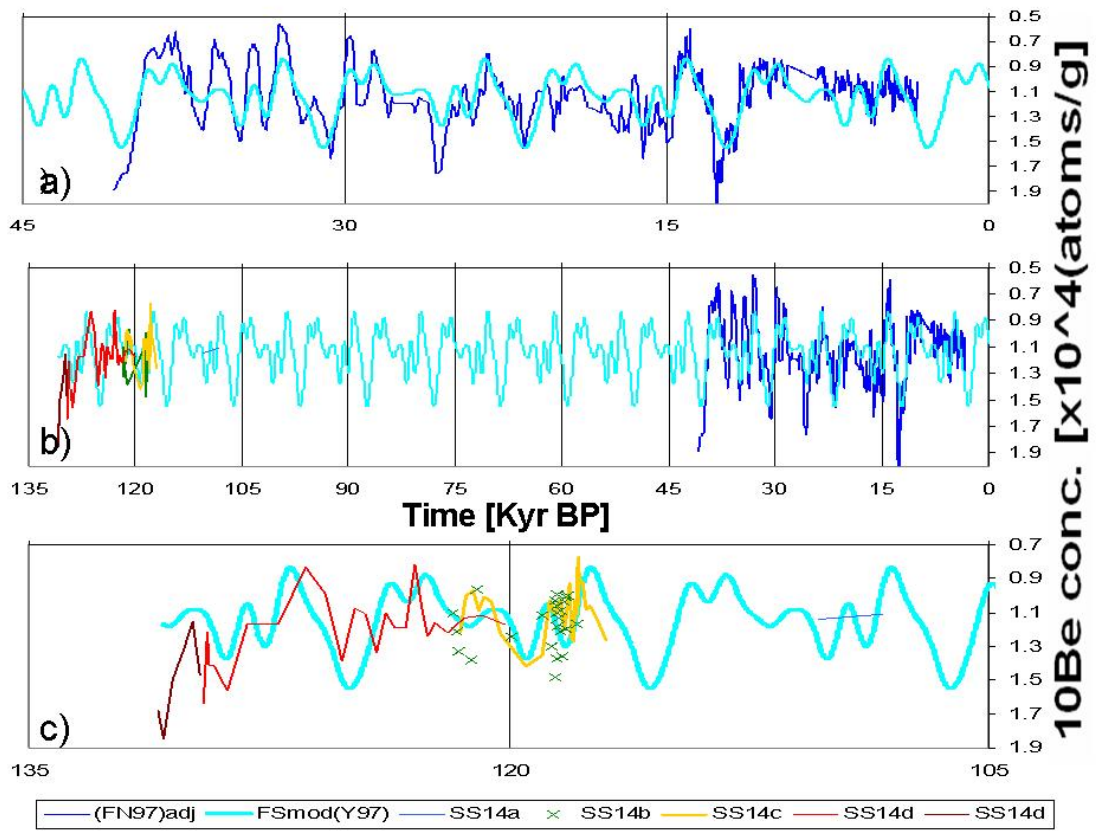
5 Figure 7. Sea level, S , reconstructed by S03, and its two models: a linear analogue
6 transformation of the CRB SAT record, with a lag of ~1500 yrs, and an analogue model based
7 on the same S03 record, with a lag of 9.6 Kyrs. The diagrams show two scales for the SL: one
8 is the original S03 SL scale (left), and the other is the adjusted scale based on a recent
9 published reconstruction (see details in Appendix D).

10



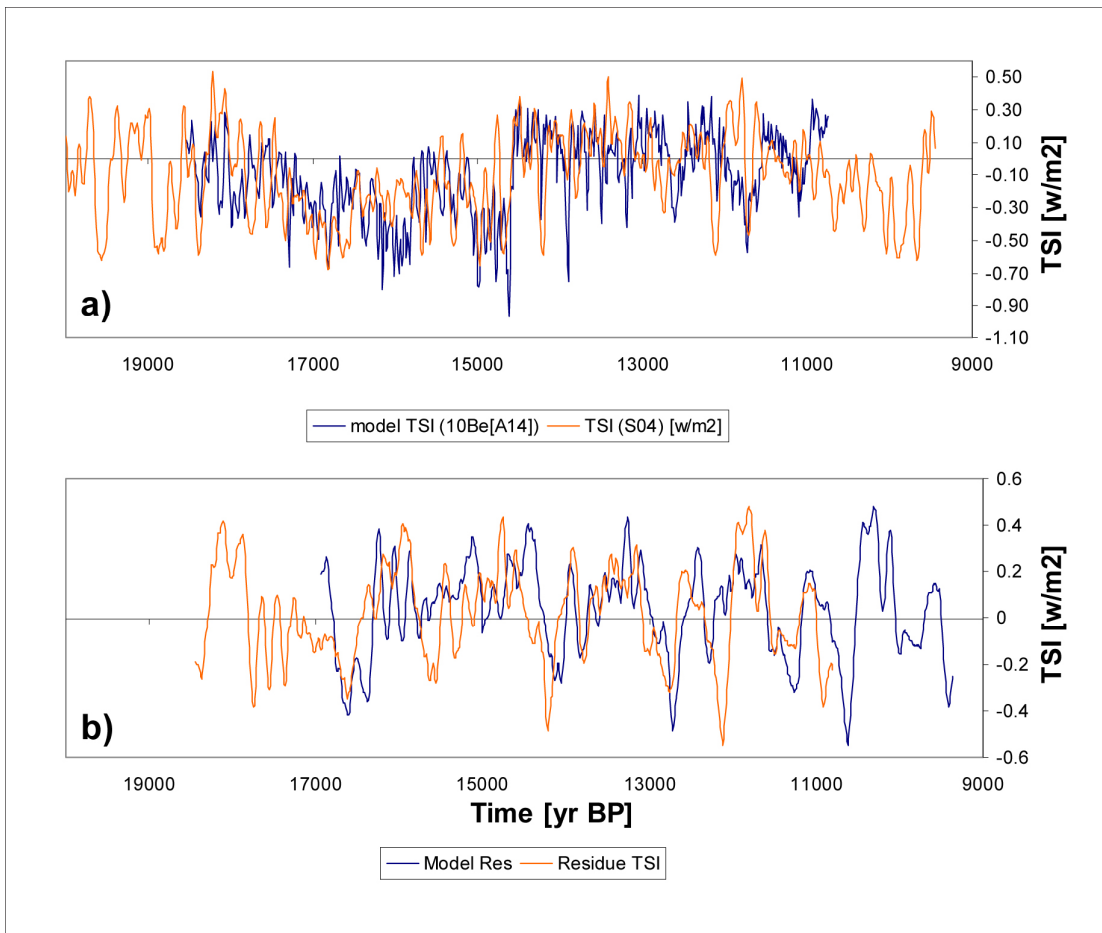
1

2 **Figure 1.**



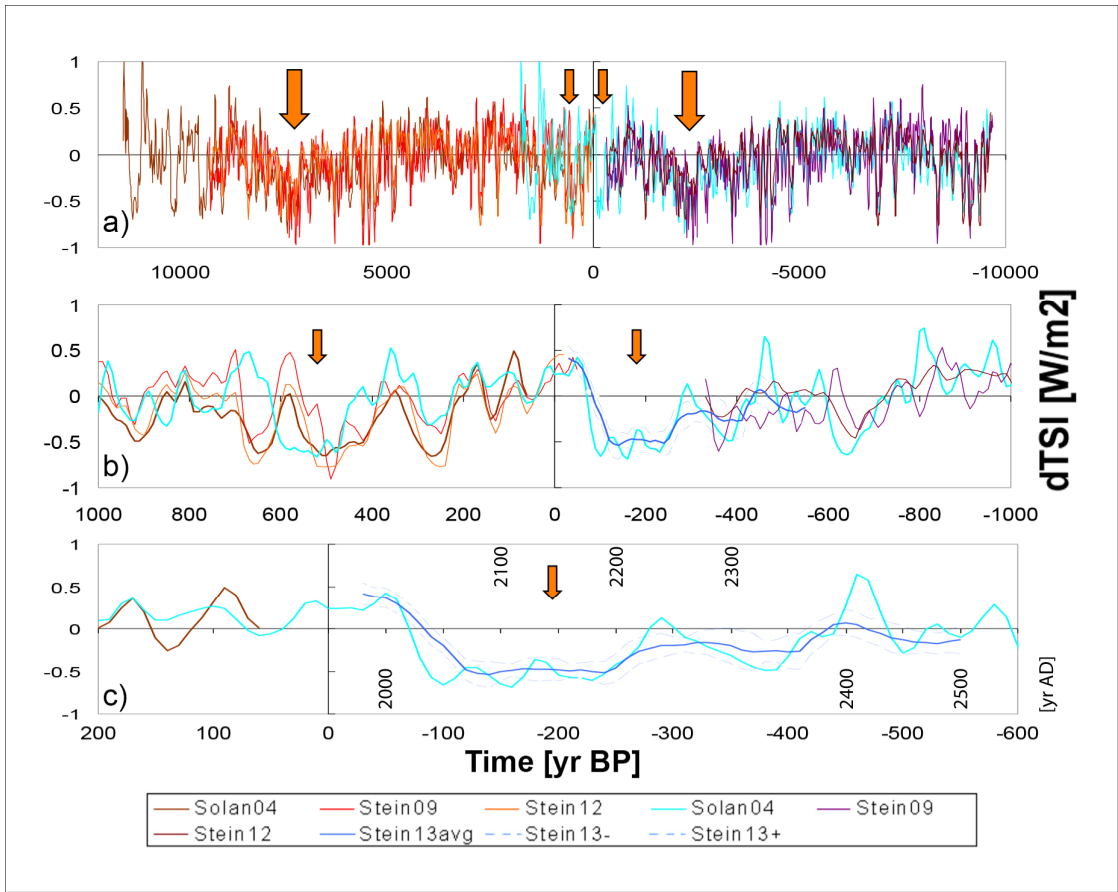
1

2 **Figure 2.**



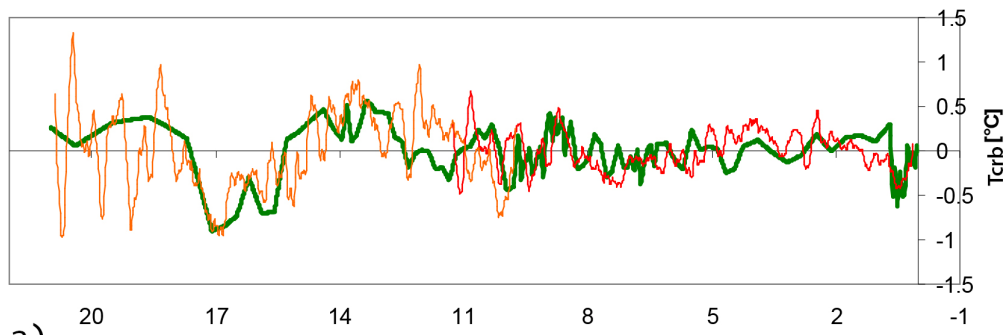
1

2 **Figure 3.**

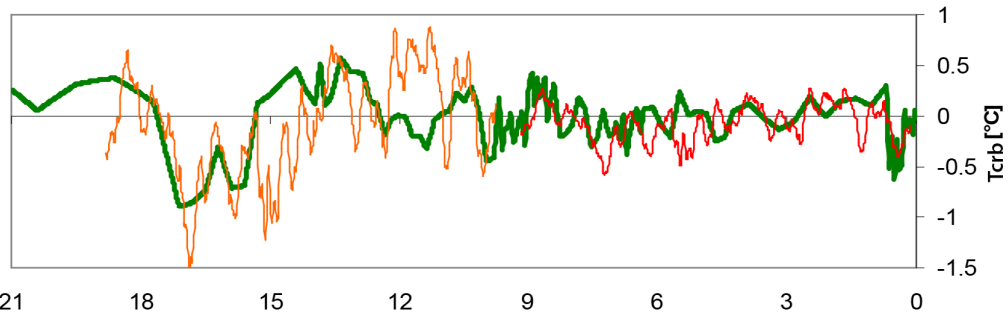


1

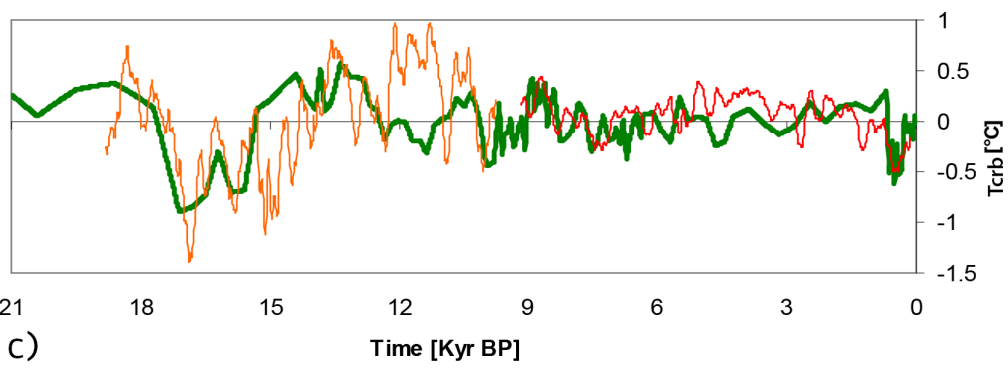
2 **Figure 4.**



a) — MATCRB det(°C) — TSI(S09) — TSI(S04)lead9Kyr



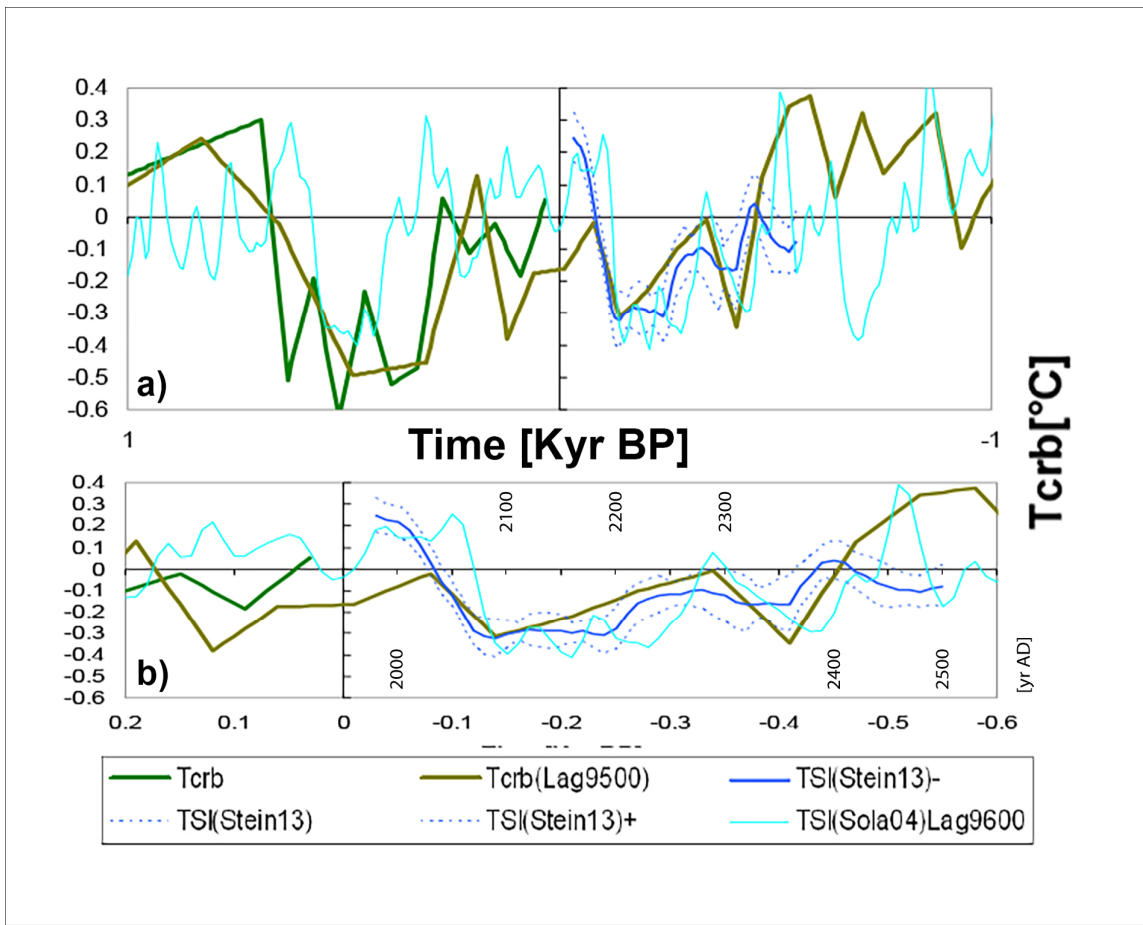
b) — MATCRB det(°C) — TSI(S09) — TSI(S09)lead9Kyr



c) — MATCRB det(°C) — TSI(S12) — TSI(S12)lead9.6Kyr

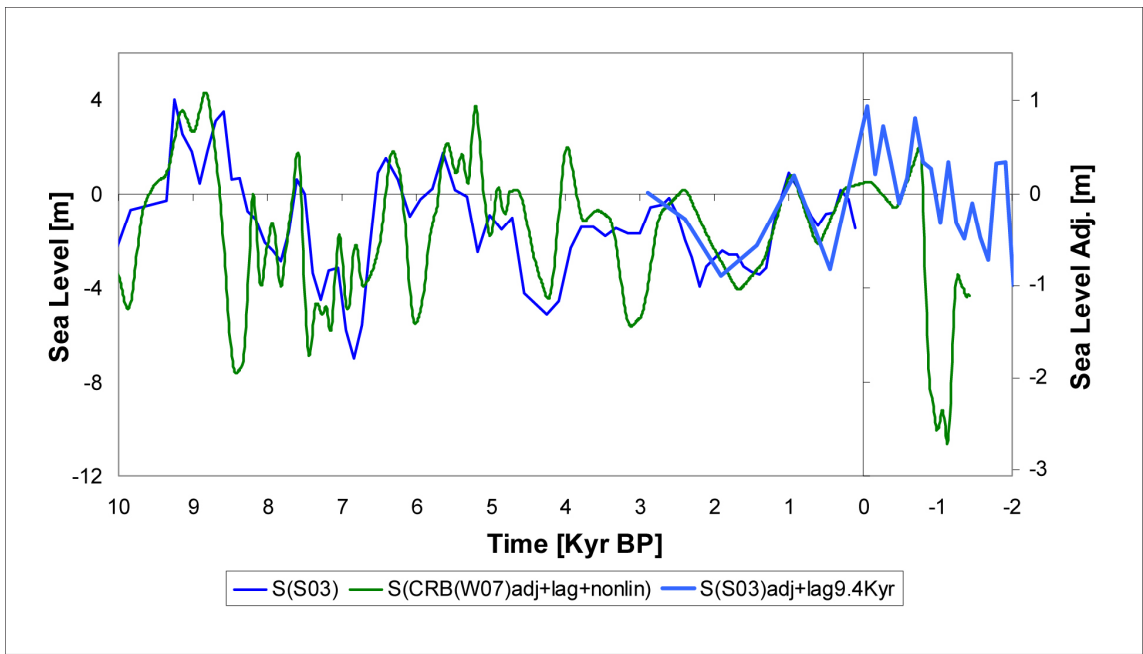
1

2 **Figure 5.**



1

2 **Figure 6.**



- 1
- 2
- 3

Figure 7.